



ALICE

Creighton
UNIVERSITY



U.S. DEPARTMENT OF
ENERGY

Office of
Science

Overview of recent UPC results from ALICE with a focus on incoherent measurements

Simone Ragoni

Creighton University, USA

A wide-angle, high-angle photograph of a large-scale industrial facility, likely a particle accelerator or detector. The scene is dominated by a complex network of metal structures, pipes, and a dense array of cables. The walls are painted a vibrant red, and the floor is a mix of metal grates and concrete. Several workers in safety gear, including hard hats and work clothes, are visible throughout the scene, engaged in various tasks. The lighting is a mix of bright white and cool blue tones. In the foreground, a large bundle of black cables is neatly organized, with some yellow and blue connectors visible. A small yellow sign with the text "AREA B" is attached to a red structure in the lower-left quadrant. The overall atmosphere is one of intense technical activity and precision engineering.

OUR UPC PHYSICS PROGRAM
IS THE FORERUNNER OF EIC

Outline



- Introduction to ultra-peripheral collisions (UPC)
- The ALICE detector
- Results on exclusive and dissociative J/ψ in p-Pb UPC
- Results on coherent and incoherent J/ψ in UPC Pb-Pb
- Measurements of the energy dependence of the photonuclear cross sections

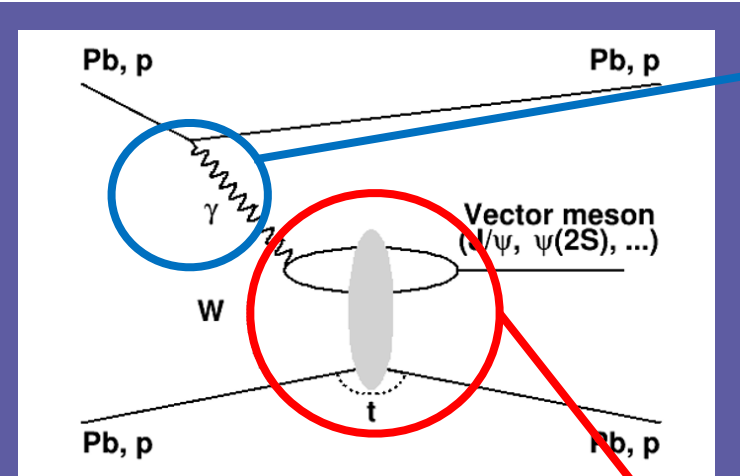
Outline



- Introduction to ultra-peripheral collisions (UPC)
- The ALICE detector
- Results on exclusive and dissociative J/ψ in p-Pb UPC
- Results on coherent and incoherent J/ψ in UPC Pb-Pb
- Measurements of the energy dependence of the photonuclear cross sections

Introduction to ultraperipheral collisions (UPC)

Only QED involved at this vertex!



- Large impact parameter (beyond the reach of the strong interaction)
- Vector meson production
- e.g. ρ^0 , J/ψ , $\psi(2S)$

$$\frac{d\sigma^T(\gamma p \rightarrow J/\Psi + p)}{dt} = \frac{|M|^2}{16\pi s^2} \text{ LO}$$

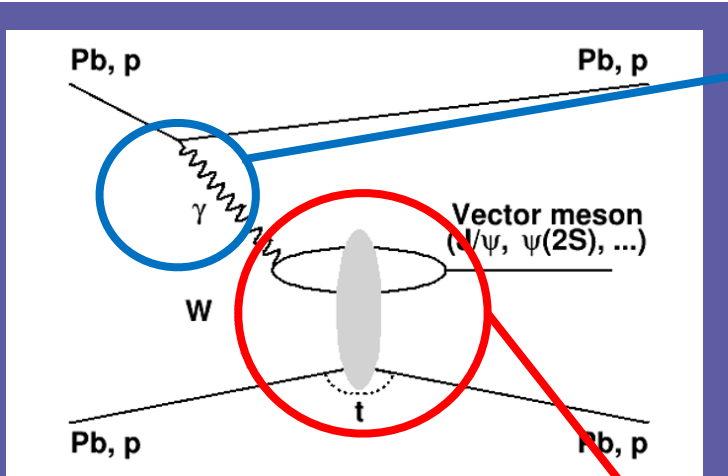
$$= [F_N^{2G}(t)]^2 \frac{\alpha_e^2 \Gamma_{ee}^J m_J^3}{3\alpha_{e.m.}} \pi^3 \left[\bar{x} G(\bar{x}, \bar{q}^2) \frac{2\bar{q}^2 - |q_t^J|^2}{(2\bar{q}^2)^3} \right]^2$$

Ryskin: Z. Phys. C 57, 89-92 (1993)

Hard scale assured by high mass states i.e. J/ψ , $\psi(2S)$

- *Coherent photoproduction:* photon couples with the **entire nucleus**
- *Incoherent photoproduction:* photon couples with a **single nucleon** only
- Different average p_T of the vector mesons for the two processes

Introduction to ultraperipheral collisions (UPC)



Only QED involved at this vertex!

$|t|$ the square of the momentum transferred between the incoming and outgoing target nucleus

W the centre-of-mass energy of the photon-target system

Hard scale assured by high mass states i.e. $J/\psi, \psi(2S)$

- Large impact parameter (beyond the reach of the strong interaction)
- Vector meson production
- e.g. $\rho^0, J/\psi, \psi(2S)$

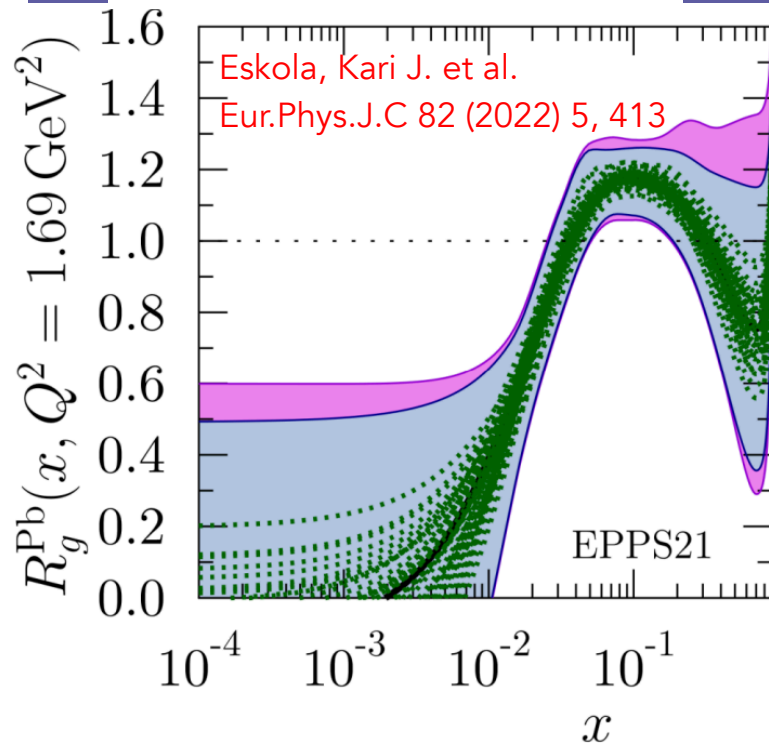
- *Coherent photoproduction:* photon couples with the **entire nucleus**
- *Incoherent photoproduction:* photon couples with a **single nucleon** only
- Different average p_T of the vector mesons for the two processes

Physics of ultra-peripheral collisions (UPC)

Studying nuclear shadowing

$$R_g^A(x, Q^2) = \frac{g_A(x, Q^2)}{A g_p(x, Q^2)} < 1$$

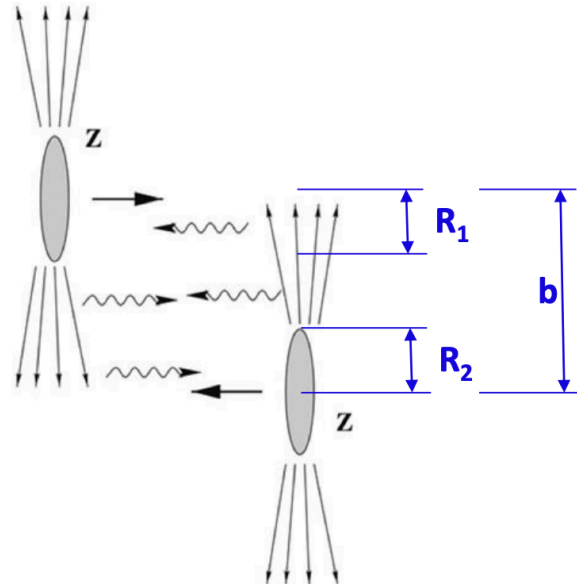
Nuclear gluon PDF
Proton gluon PDF



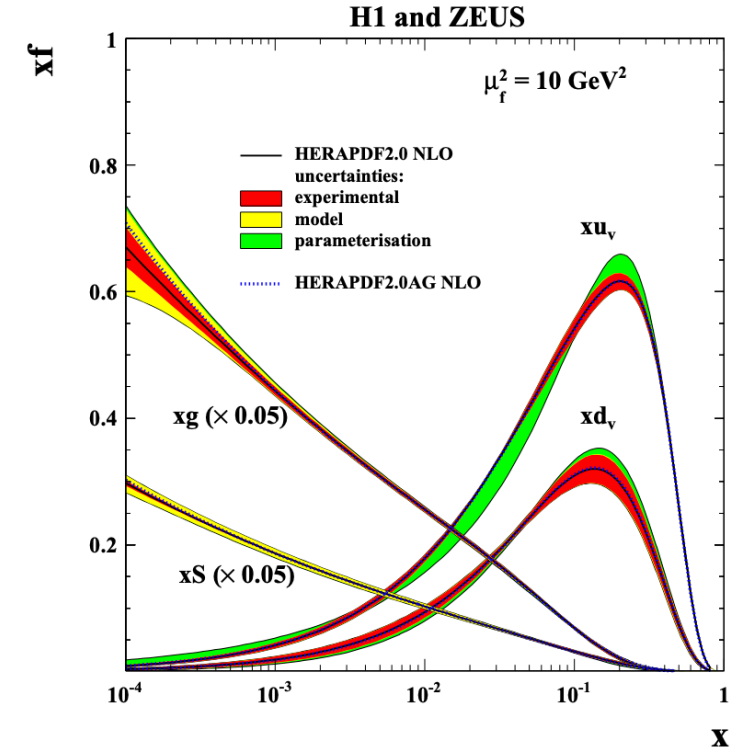
$$\frac{d\sigma^T(\gamma p \rightarrow J/\Psi + p)}{dt} = \frac{|M|^2}{16\pi s^2} \text{ LO}$$

$$= [F_N^{2G}(t)]^2 \frac{\alpha_e^2 \Gamma_{ee}^J m_J^3}{3\alpha_{e.m.}} \pi^3 \left[\bar{x} G(\bar{x}, \bar{q}^2) \frac{2\bar{q}^2 - |q_t^J|^2}{(2\bar{q}^2)^3} \right]^2$$

Ryskin: Z. Phys. C 57, 89-92 (1993)



Looking for gluon saturation



H1 and Zeus, EPCJ 75 (2015) 580

Outline



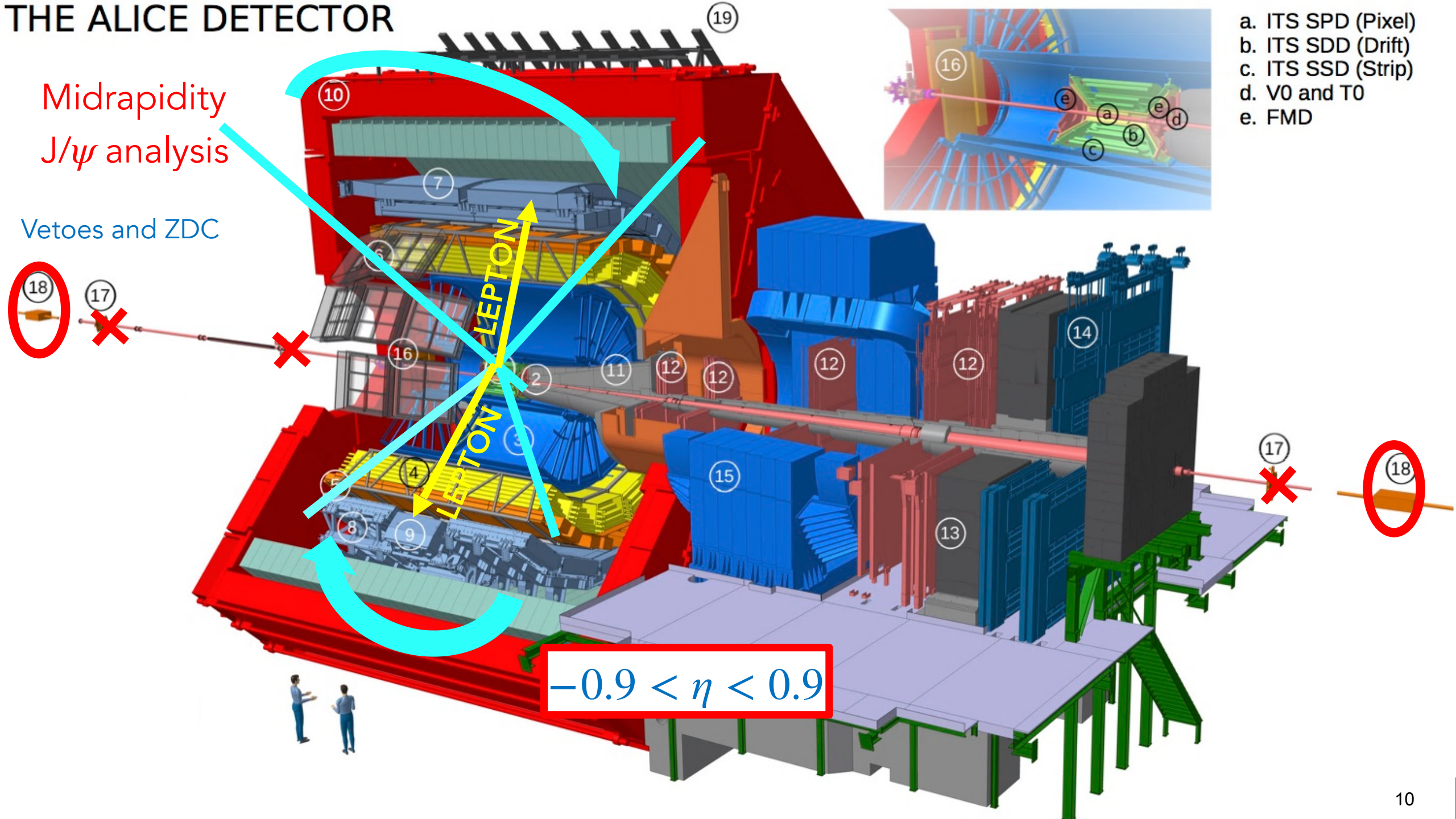
- Introduction to ultra-peripheral collisions (UPC)
- The ALICE detector
- Results on exclusive and dissociative J/ψ in p-Pb UPC
- Results on coherent and incoherent J/ψ in UPC Pb-Pb
- Measurements of the energy dependence of the photonuclear cross sections

THE ALICE DETECTOR

Midrapidity
 J/ψ analysis

Vetoos and ZDC

- a. ITS SPD (Pixel)
- b. ITS SDD (Drift)
- c. ITS SSD (Strip)
- d. V0 and T0
- e. FMD



$$-0.9 < \eta < 0.9$$

Outline

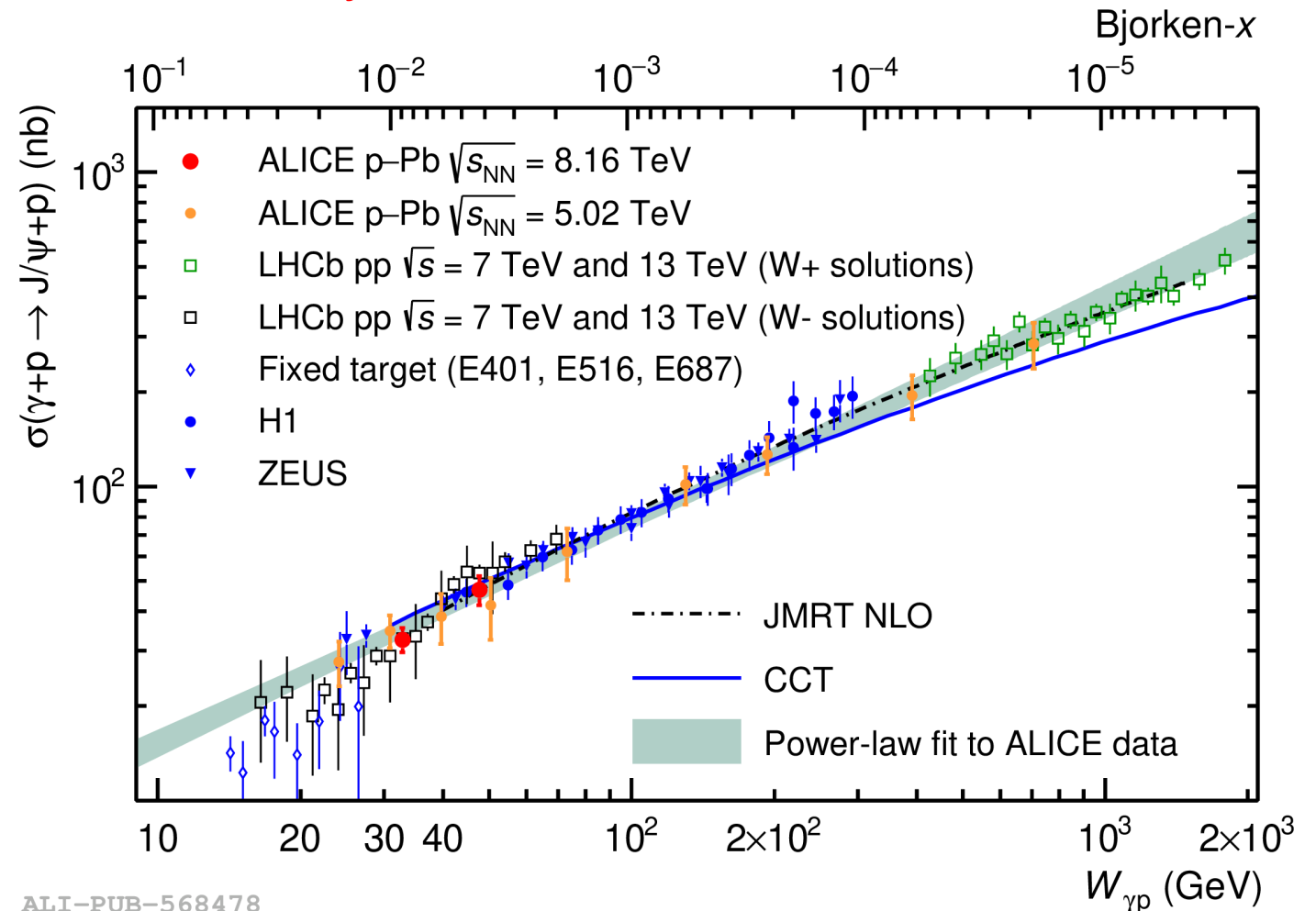


- Introduction to ultra-peripheral collisions (UPC)
- The ALICE detector
- Results on exclusive and dissociative J/ψ in p-Pb UPC
- Results on coherent and incoherent J/ψ in UPC Pb-Pb
- Measurements of the energy dependence of the photonuclear cross sections

Exclusive J/ψ in p-Pb

- $x = e^{\pm|y|} \frac{M_{J/\psi}}{2E_p}$
- Probing Bjorken- $x \sim 10^{-5}$ with ALICE
- power-law growth of cross-sections \rightarrow power-law growth of gluon distributions down to $x \sim 10^{-6}$ \rightarrow no clear signs of gluon saturation
- ALICE points: forward, semiforward and midrapidity configurations
 - Forward: two muons in the spectrometer
 - Semiforward: one in the spectrometer, one in the central barrel
 - Midrapidity: two muons/electrons in the central barrel

ALICE, *Phys.Rev.D* 108 (2023) 11, 112004



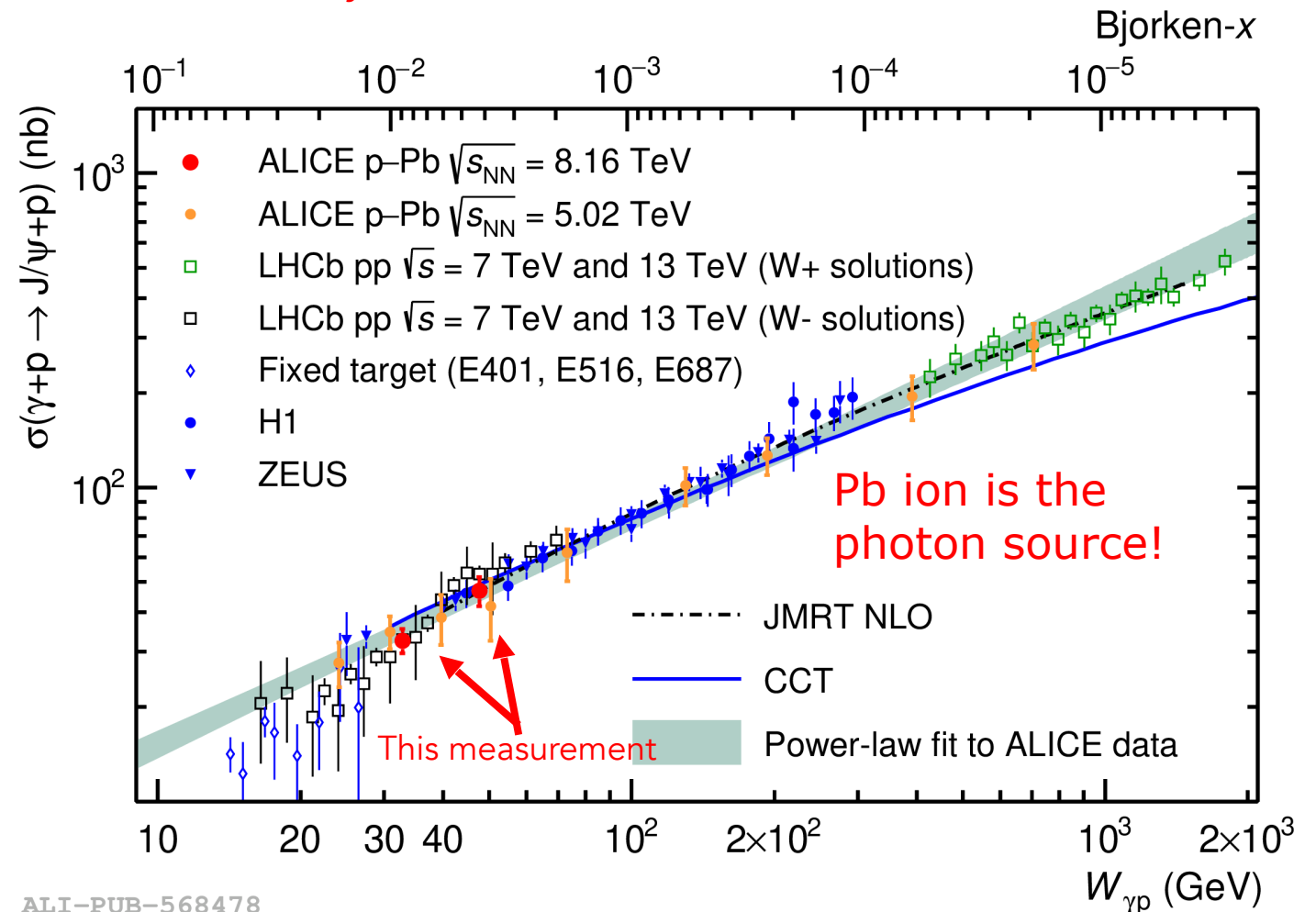
ALI-PUB-568478

Eur. Phys. J. C (2019) 79: 402 (ALICE midrapidity and semiforward),
 Phys. Rev. Lett. 113 no. 23, (2014) 232504 (ALICE forward)

Exclusive J/ψ in p-Pb

- $x = e^{\pm|y|} \frac{M_{J/\psi}}{2E_p}$
- Probing Bjorken- $x \sim 10^{-5}$ with ALICE
- power-law growth of cross-sections \rightarrow power-law growth of gluon distributions down to $x \sim 10^{-6}$ \rightarrow no clear signs of gluon saturation
- ALICE points: forward, semiforward and midrapidity configurations
 - Forward: two muons in the spectrometer
 - Semiforward: one in the spectrometer, one in the central barrel
 - Midrapidity: two muons/electrons in the central barrel

ALICE, *Phys.Rev.D* 108 (2023) 11, 112004



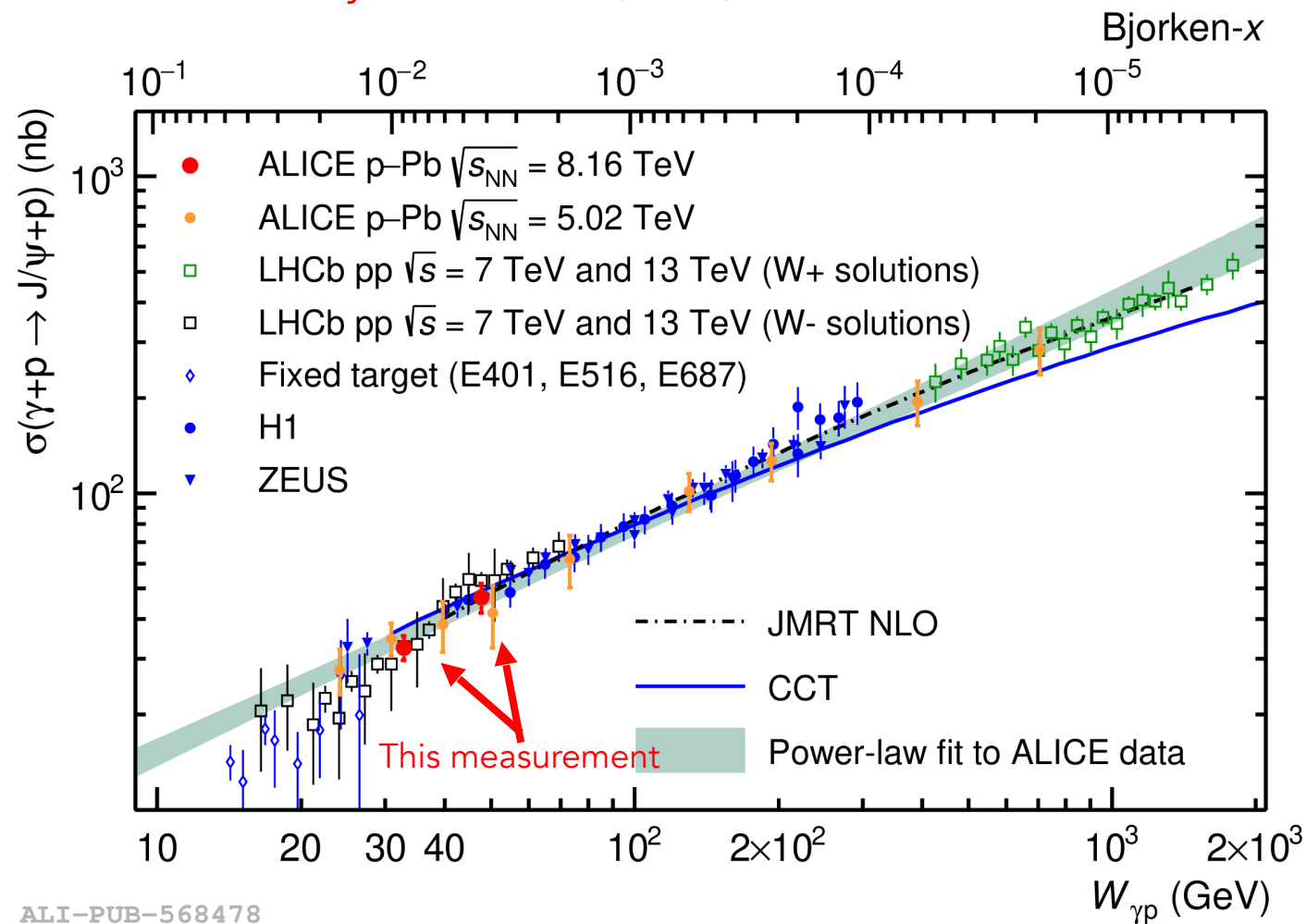
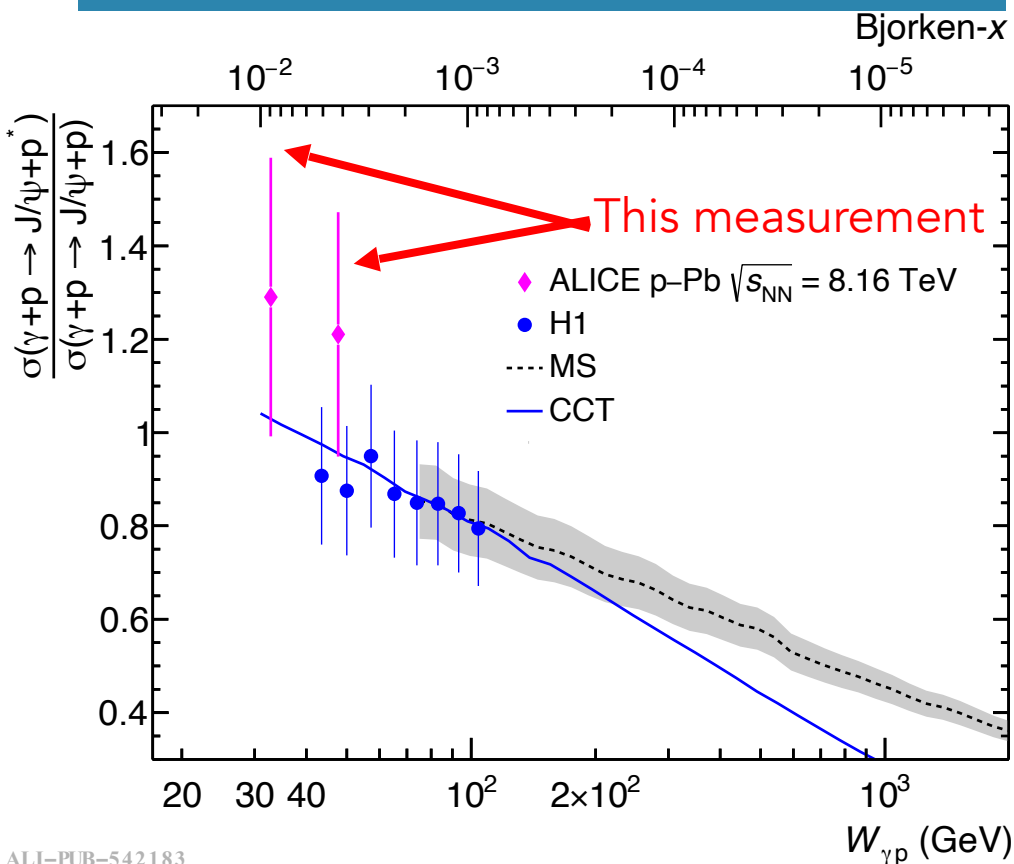
ALI-PUB-568478

Eur. Phys. J. C (2019) 79: 402 (ALICE midrapidity and semiforward),
 Phys. Rev. Lett. 113 no. 23, (2014) 232504 (ALICE forward)

Exclusive and dissociative J/ψ in p-Pb

ALICE, *Phys.Rev.D* 108 (2023) 11, 112004

- First result at the LHC of the measurement of dissociative J/ψ



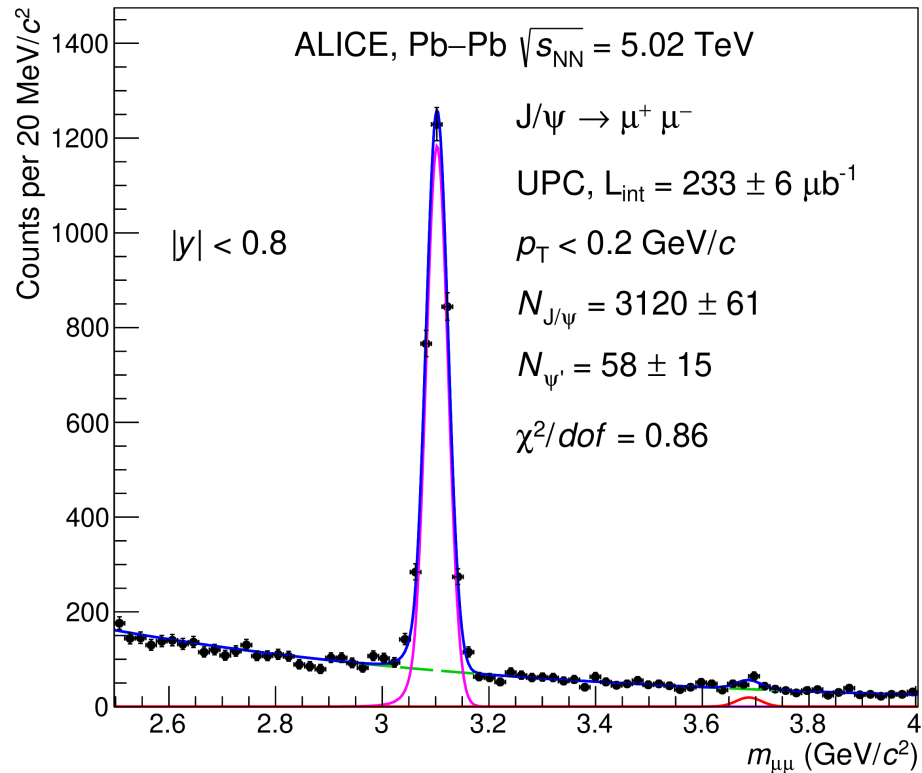
ALI-PUB-568478

Outline

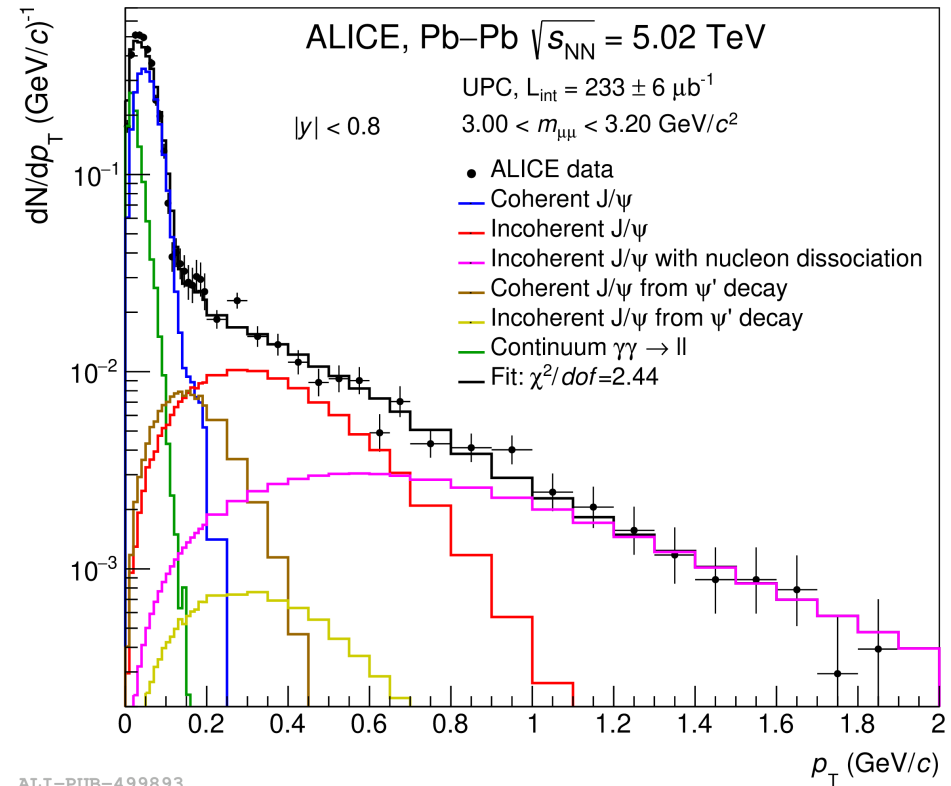


- Introduction to ultra-peripheral collisions (UPC)
- The ALICE detector
- Results on exclusive and dissociative J/ψ in p-Pb UPC
- Results on coherent and incoherent J/ψ in UPC Pb-Pb
- Measurements of the energy dependence of the photonuclear cross sections

Coherent vs incoherent J/ψ



ALI-PUB-499888



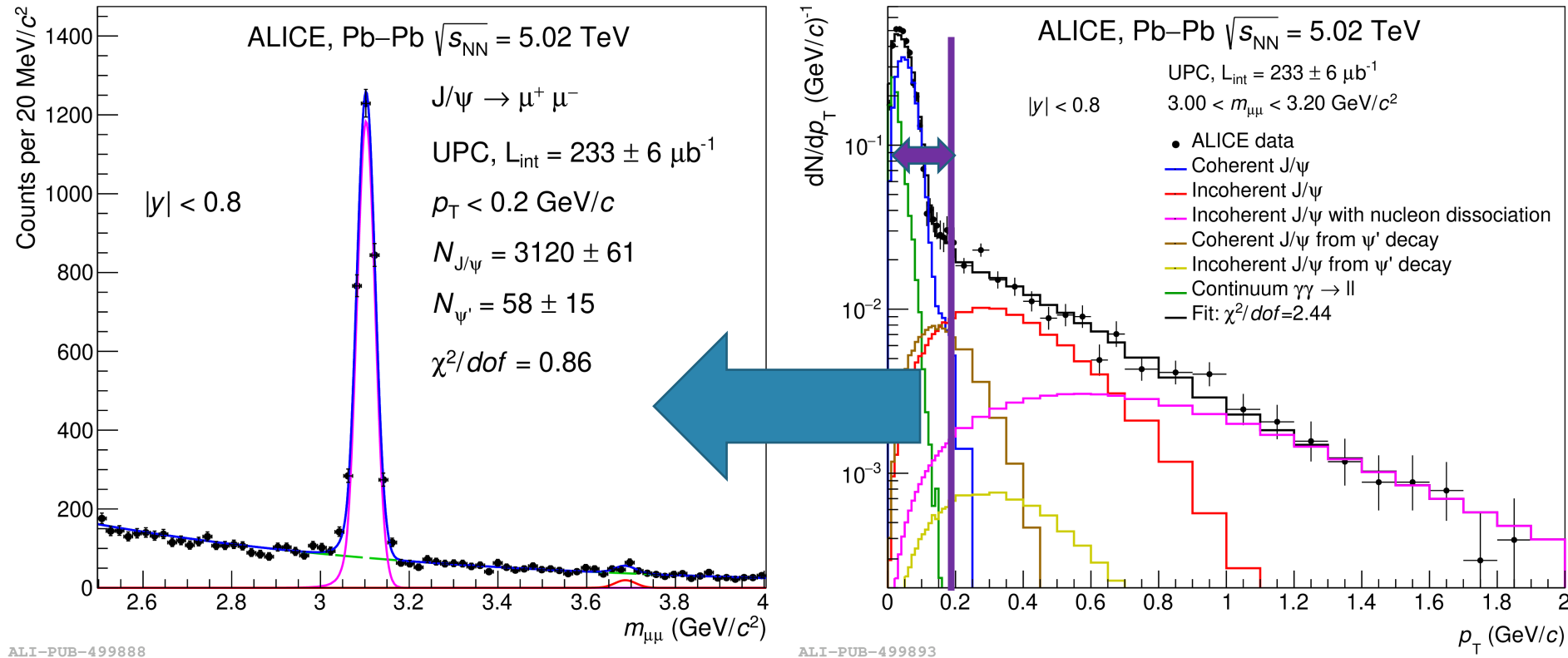
ALI-PUB-499893

Plots at midrapidity

ALICE, Eur. Phys. J. C 81 (2021) 712

- Coherent (dimuon $p_T < 0.2$ GeV/c) – photon couples to entire nucleus *coherently*
- Incoherent J/ψ features a much wider p_T distribution – photon interacts with a single nucleon of the target nucleus

Coherent vs incoherent J/ψ



Plots at
midrapidity

ALICE, Eur.
Phys. J. C
81 (2021)
712

- Coherent (dimuon $p_T < 0.2 \text{ GeV}/c$) – photon couples to entire nucleus *coherently*
- Incoherent J/ψ features a much wider p_T distribution – photon interacts with a single nucleon of the target nucleus

Studying coherent J/ψ in terms of...

1. Angular distributions
2. y
3. p_T^2
4. $W_{\gamma Pb,n}^2 = m\sqrt{s_{NN}}e^{-y}$

Studying coherent J/ψ in terms of...

1. Angular distributions

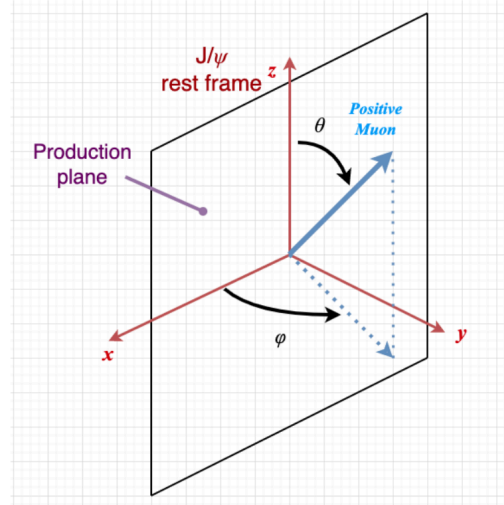
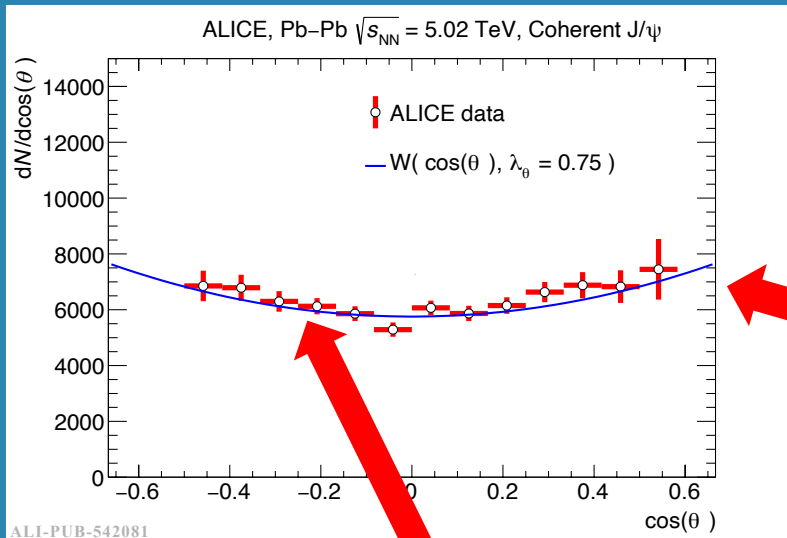
2. y

3. p_T^2

4. $W_{\gamma Pb,n}^2 = m\sqrt{s_{NN}}e^{-y}$

Coherent J/ψ polarisation

- Quasireal photons ($Q^2 \sim 0$): s-channel helicity conservation suggests transverse polarisation for the vector meson
- Agreement with H1 (photoprod.)
- ZEUS measures electroprod.

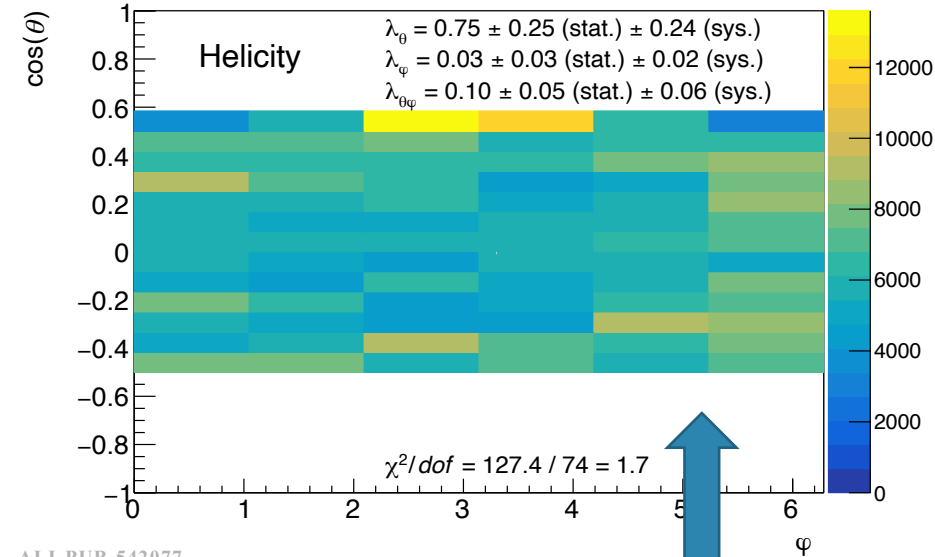


$$r_{00}^{04} = \frac{1 - \lambda_\theta}{3 + \lambda_\theta}$$

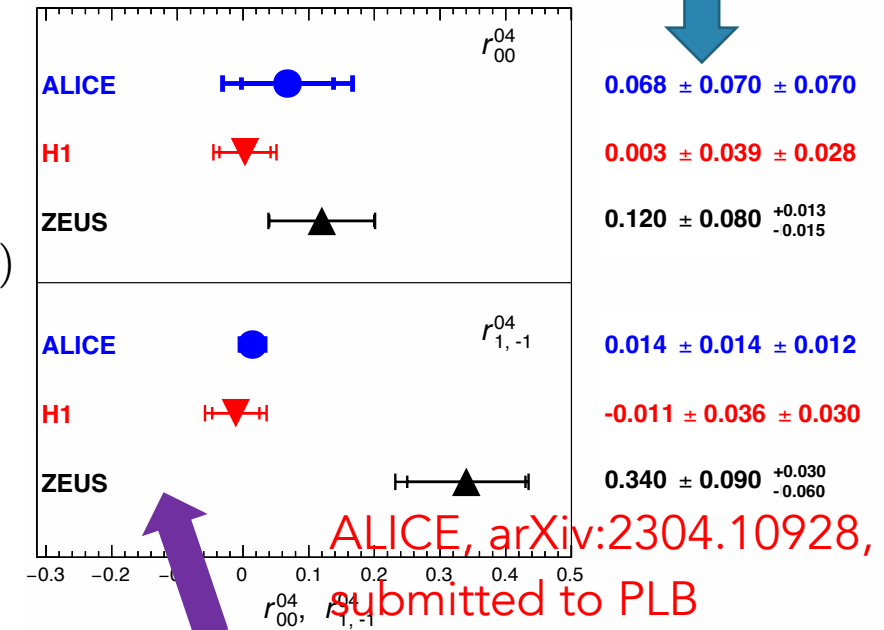
$$r_{1,-1}^{04} = \frac{\lambda_\varphi}{2} \cdot (1 + r_{00}^{04})$$

Upward parabolic shape in $\cos(\theta)$ typical of transverse polarisation

ALICE, Pb-Pb $\sqrt{s_{NN}} = 5.02$ TeV, coherent J/ψ



ALI-PUB-542077



ALICE, arXiv:2304.10928, submitted to PLB

ALI-PUB-542093

Results with the spin-density matrix elements

$$W(\cos \theta, \varphi) \propto \frac{1}{3 + \lambda_\theta} \cdot [1 + \lambda_\theta \cdot \cos^2 \theta + \lambda_\varphi \cdot \sin^2 \theta \cdot \cos 2\varphi + \lambda_{\theta\varphi} \cdot \sin 2\theta \cos \varphi]$$

Studying coherent J/ψ in terms of...

1. Angular distributions

2. y

3. p_T^2

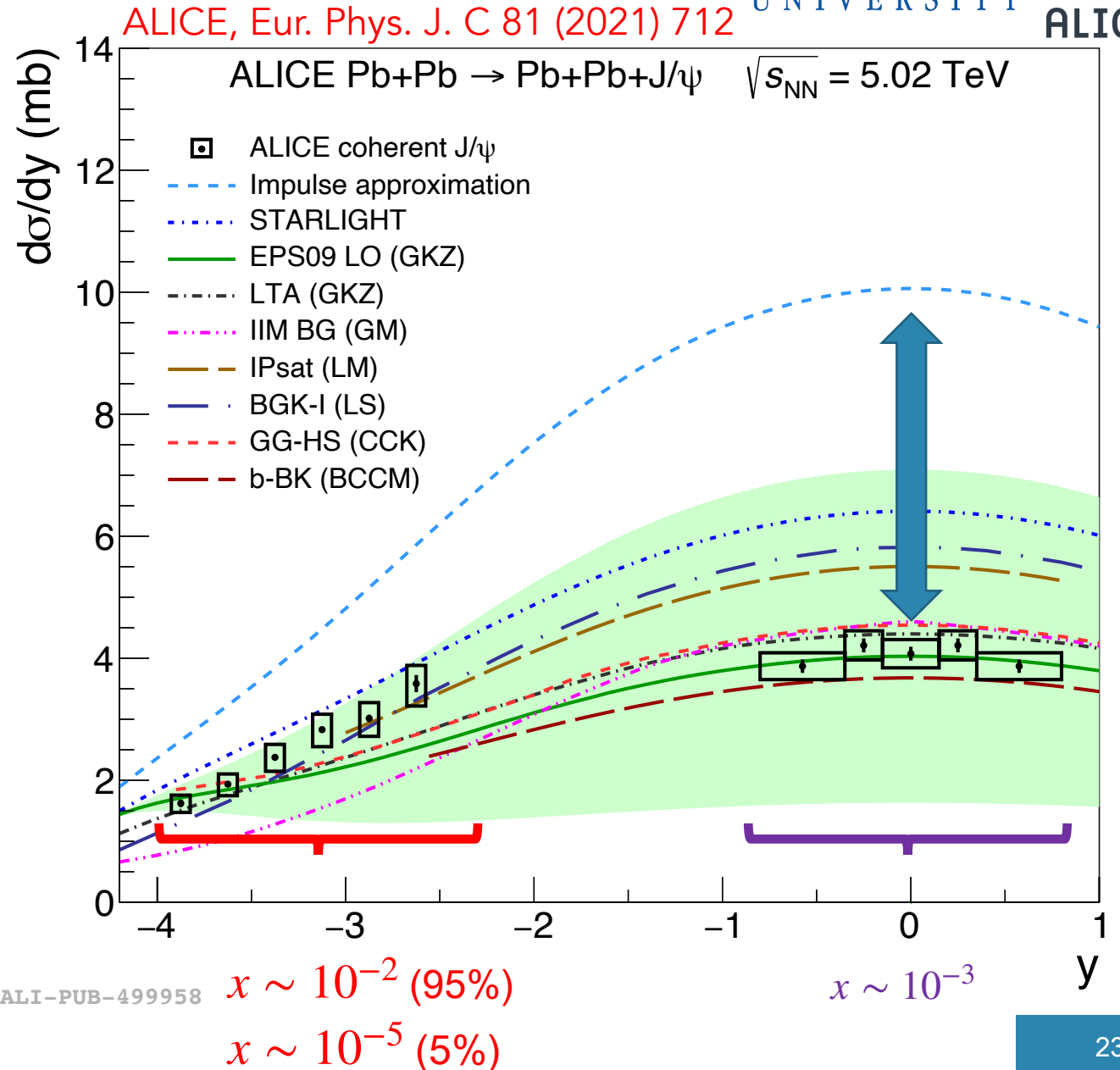
4. $W_{\gamma Pb,n}^2 = m\sqrt{s_{NN}}e^{-y}$

Coherent J/ψ cross section

- ALICE data exhibit moderate nuclear shadowing
- Nuclear suppression factor

$$S_{Pb}(y \sim 0) = \sqrt{\frac{d\sigma}{dy}_{data} / \frac{d\sigma}{dy}_{IA}} = 0.64 \pm 0.04$$

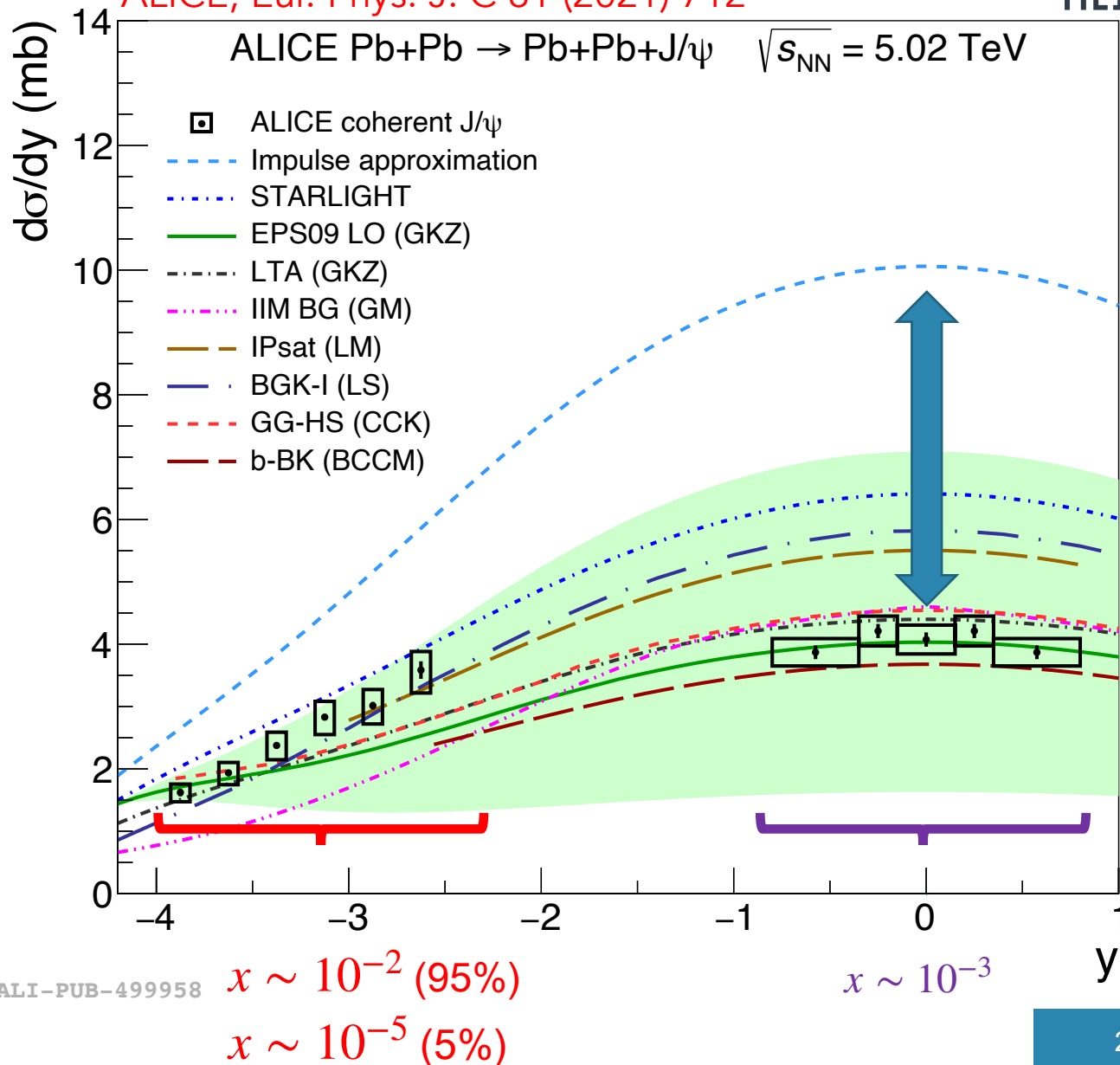
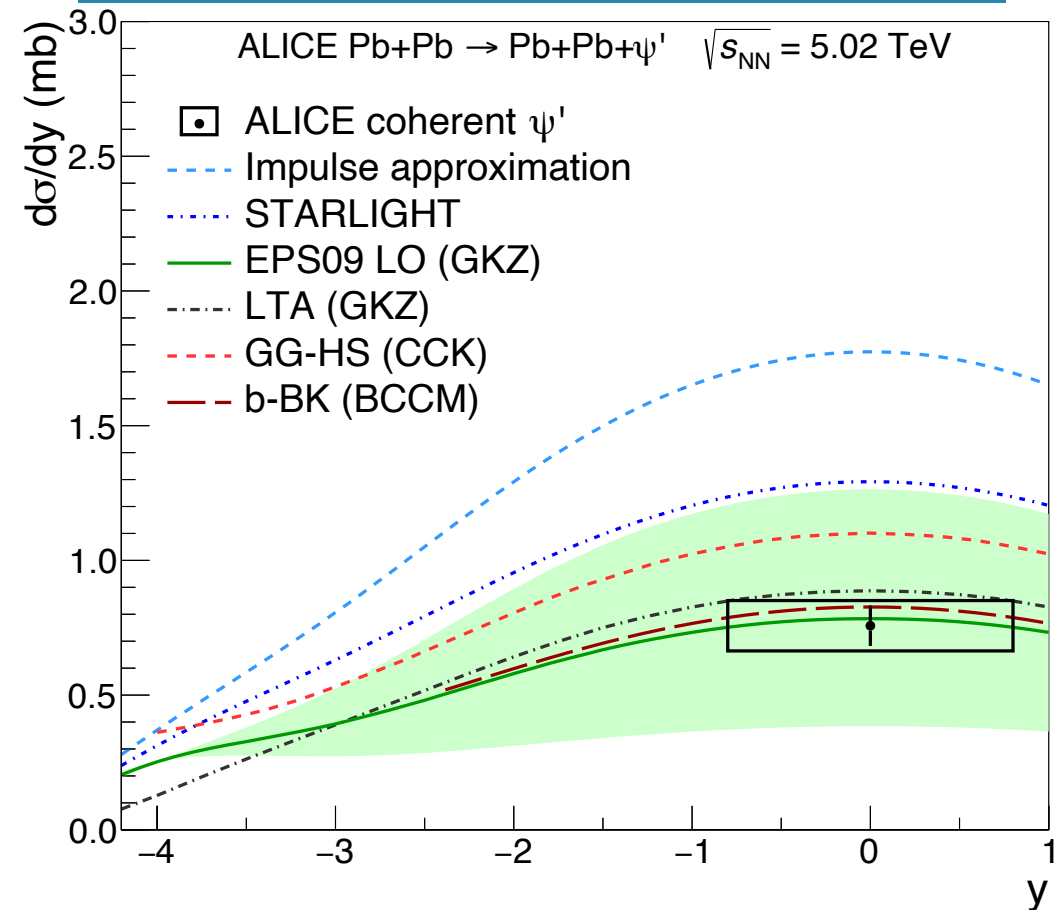
- IA = impulse approximation (no nuclear effects)
- $S(W_{\gamma p})$ - nuclear suppression factor - provides a way to test the consistency of the data with the available nuclear and nucleon PDFs and to measure the nuclear shadowing factor



Coherent J/ψ and ψ' cross section

ALICE, Eur. Phys. J. C 81 (2021) 712

$$S_{Pb}(y \sim 0, \psi') = \sqrt{\frac{d\sigma}{dy}_{data} / \frac{d\sigma}{dy}_{IA}} = 0.66 \pm 0.06$$



ALI-PUB-499958

Studying coherent J/ψ in terms of...

1. Angular distributions

2. y

3. p_T^2

4. $W_{\gamma Pb,n}^2 = m\sqrt{s_{NN}}e^{-y}$

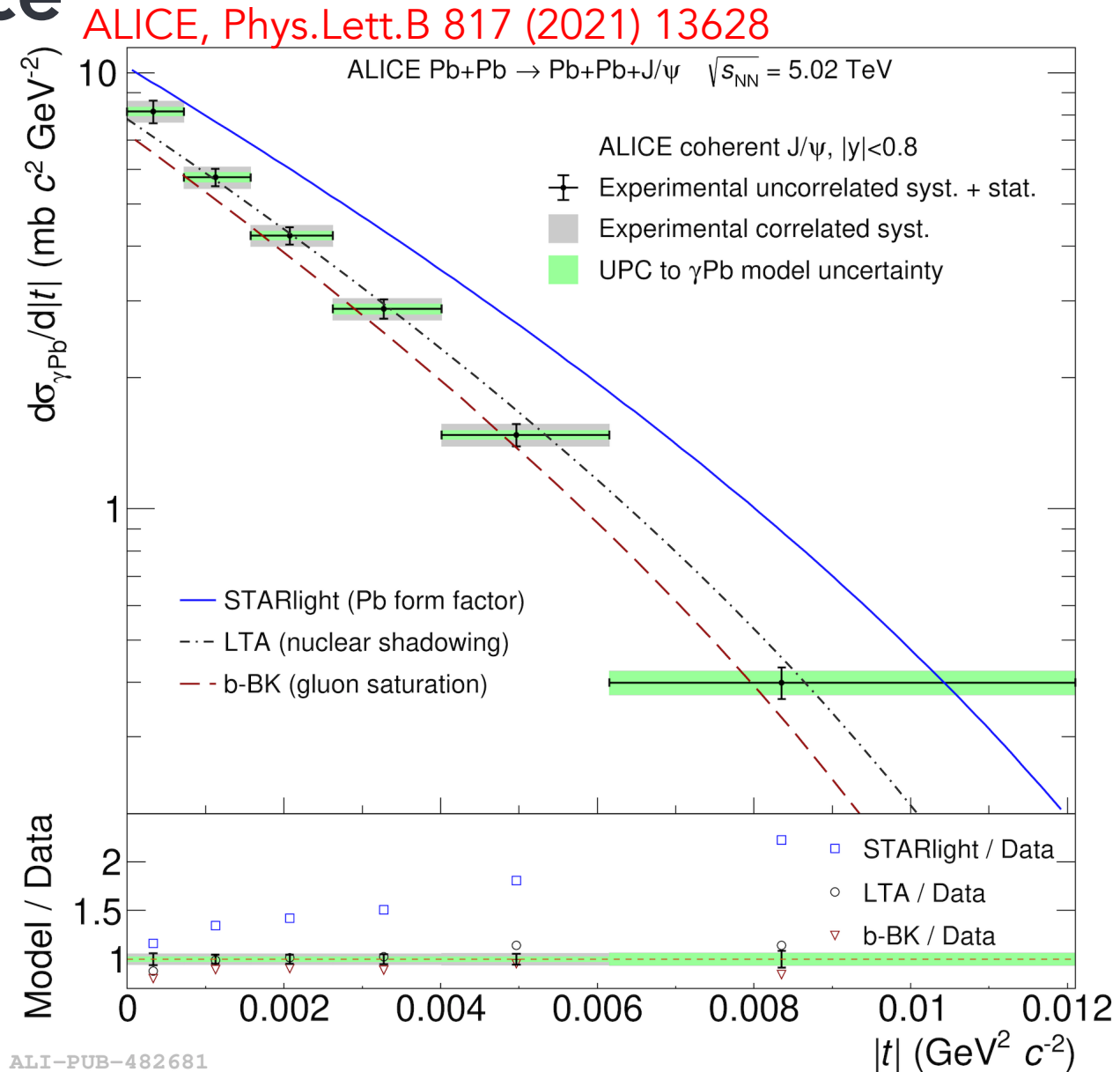
Coherent J/ψ t -dependence

$$0 < |t| < 0.012 \text{ GeV}^2$$

- From p_T^2 -dependent photoproduction to $|t|$ -dependent photonuclear production

$$\left. \frac{d^2 \sigma_{J/\psi}^{\text{coh}}}{dy dp_T^2} \right|_{y=0} = 2n_{\gamma\text{Pb}}(y=0) \frac{d\sigma_{\gamma\text{Pb}}}{d|t|}$$

- Transverse momentum of the photon accounted for by unfolding with a response matrix built from p_T^2 - and $|t|$ -distributions
- Probing the transverse gluonic structure of the nucleus at low x
- Models including QCD dynamical effects are favoured
- Run 3 data will also allow to push further in $|t|$



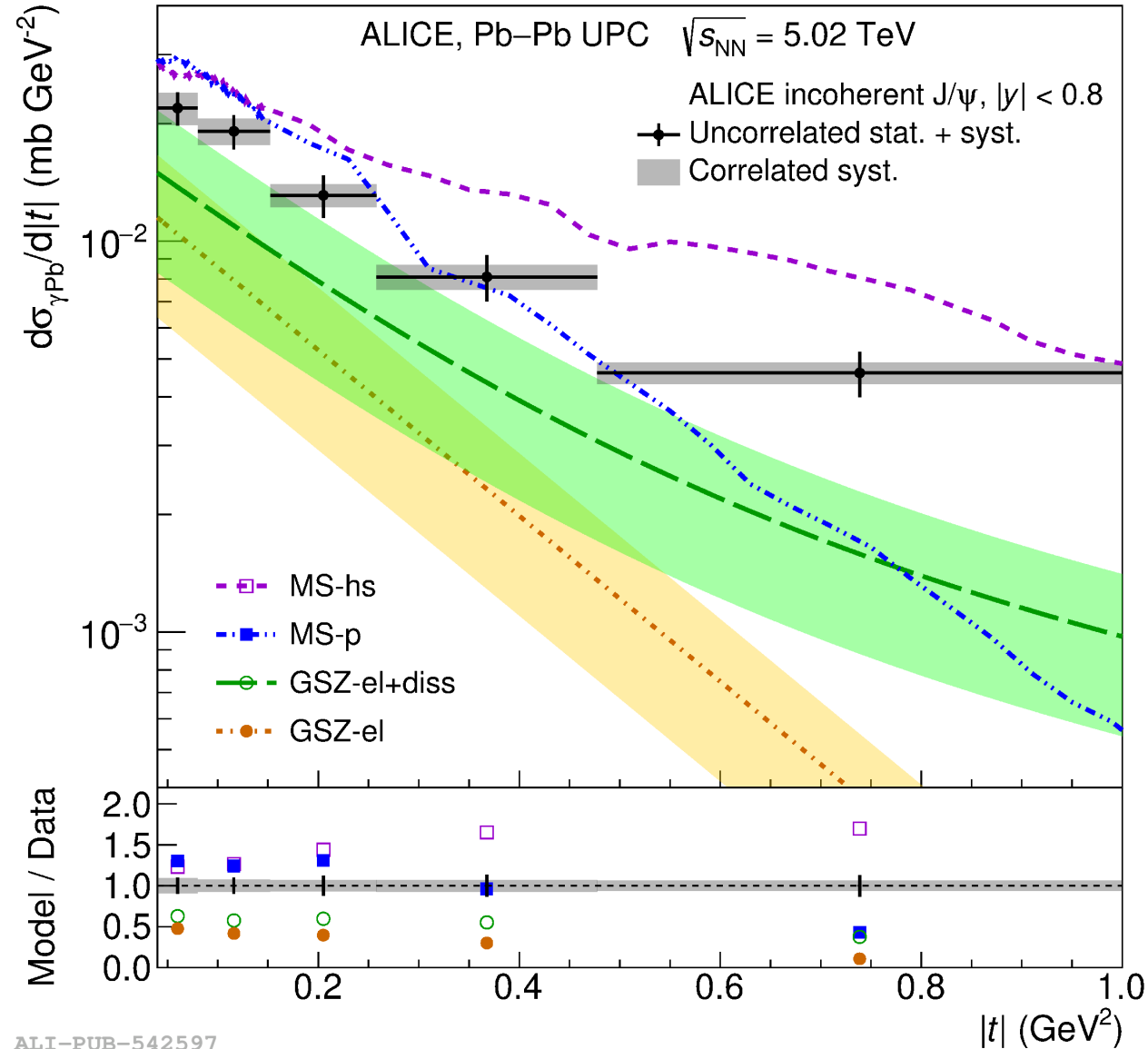
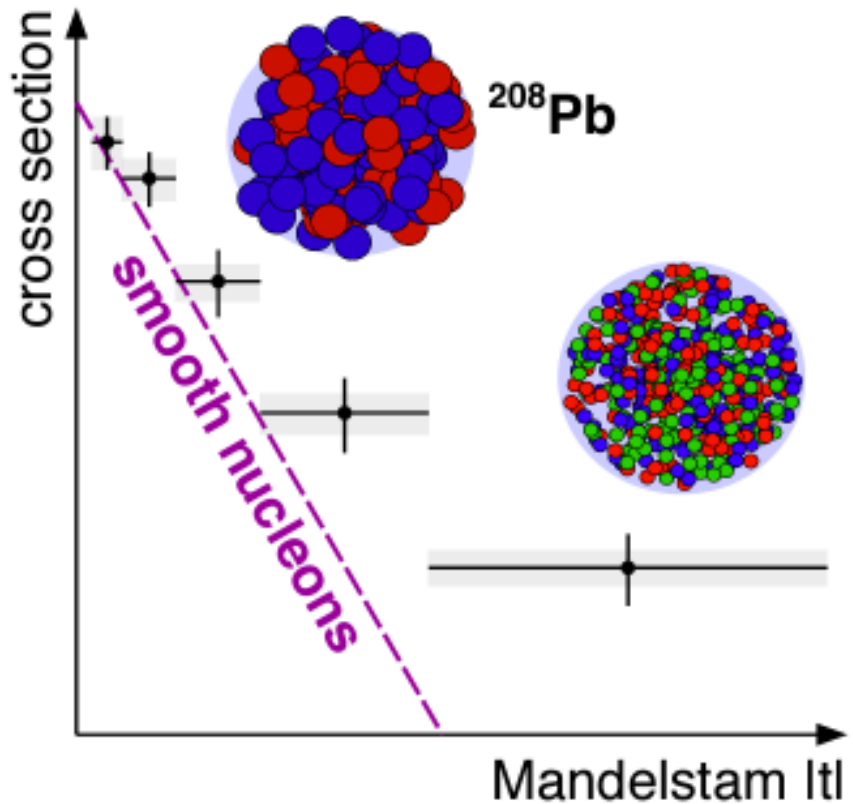
ALI-PUB-482681

Incoherent J/ψ t-dependence

$$0.04 < |t| < 1 \text{ GeV}^2$$

ALICE, *PRL* 132 (2024) 16, 162302

- Gluonic subnucleon fluctuations needed to describe the data
- First measurement of this kind ever!
- Models fail to predict normalisation



ALI-PUB-542597

Complete view of J/ψ t -dependence

- The first observation of subnucleonic structure in the Pb target using UPCs
- ALICE covers three orders of magnitude in $|t|$ with a HERA-like accuracy

H. Mäntysaari, B. Schenke / *Physics Letters B* 772 (2017) 832–838

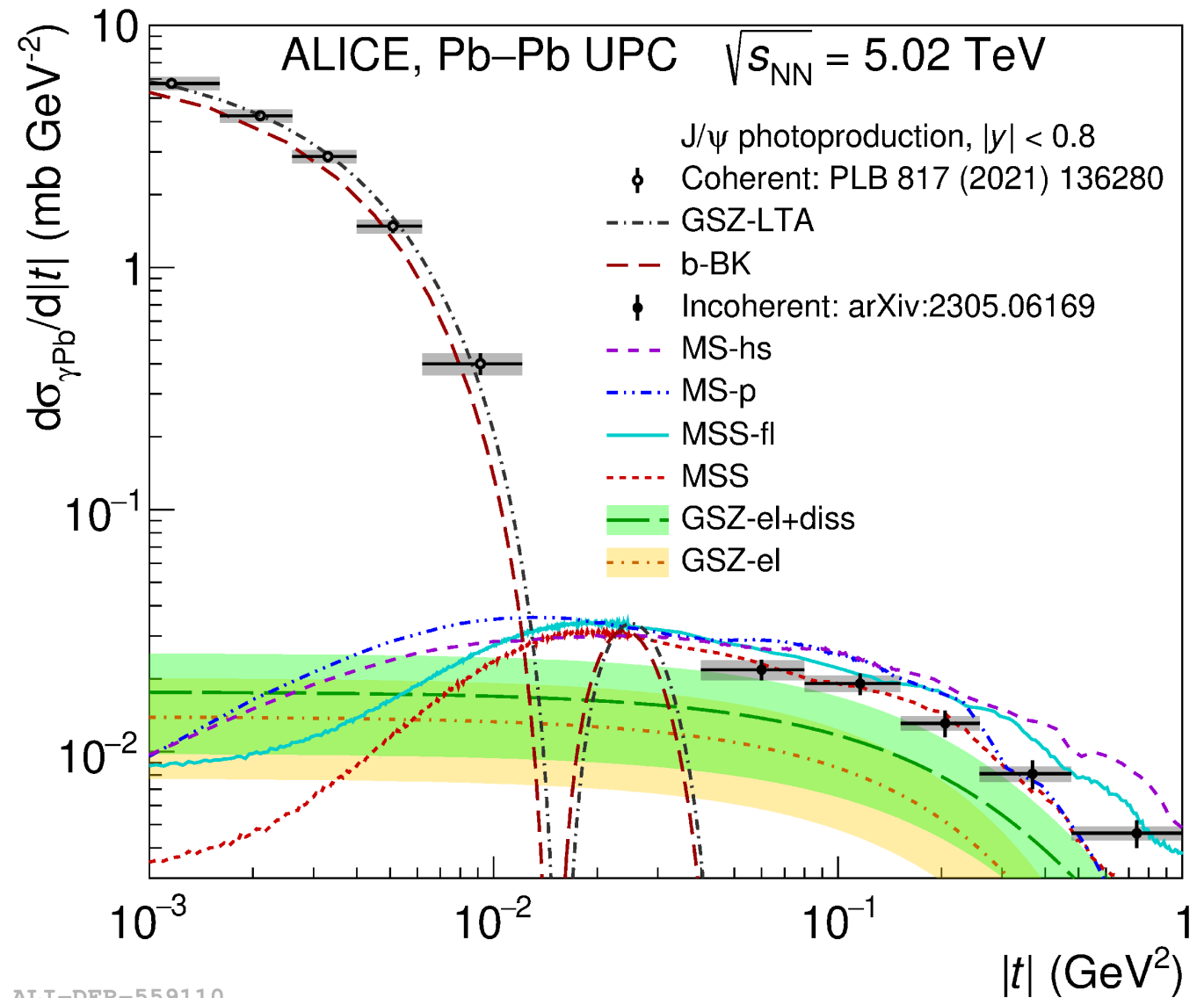
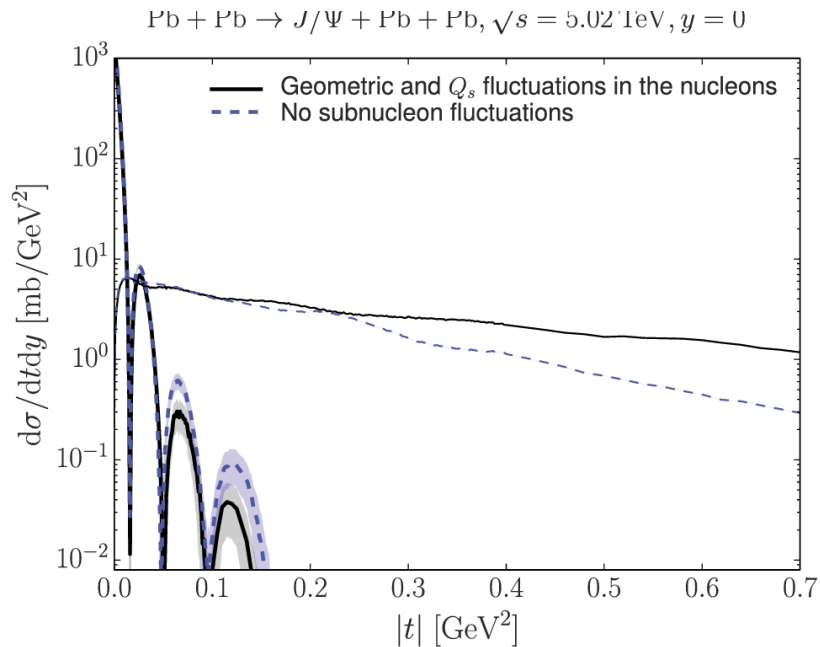


Fig. 1. Coherent (thick) and incoherent (thin lines) diffractive J/ψ production cross section as a function of t , with (solid lines) and without (dashed lines) subnucleonic fluctuations. The band shows statistical uncertainty of the calculation.

ALI-DER-559110

Studying coherent J/ψ in terms of...

1. Angular distributions
2. y
3. p_T^2
4. $W_{\gamma Pb,n}^2 = m\sqrt{s_{NN}}e^{-y}$

Outline

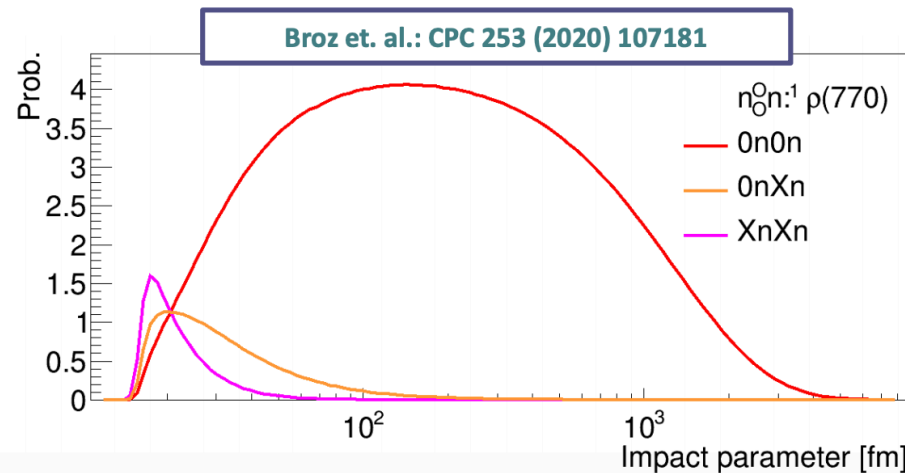


- Introduction to ultra-peripheral collisions (UPC)
- The ALICE detector
- Results on exclusive and dissociative J/ψ in p-Pb UPC
- Results on coherent and incoherent J/ψ in UPC Pb-Pb
- Measurements of the energy dependence of the photonuclear cross sections

Techniques for the photon direction ambiguity

Neutron emission:

- $x = \frac{M_{VM}}{\sqrt{s_{NN}}} \cdot e^{\pm y}$
- Ambiguity due to sign in the rapidity of the photon emitter $\rightarrow 10^{-2}, 10^{-5}$



- Using the neutron ZDCs on the A and C side to detect the neutrons!
- E.g. 0N0N: no neutrons on either ZDCs
- E.g. 0NXN: neutrons only on one side

$$\frac{d\sigma_{PbPb}^{0N0N}}{dy} = n_{0N0N}(\gamma, +y) \cdot \sigma_{\gamma Pb}(+y) + n_{0N0N}(\gamma, -y) \cdot \sigma_{\gamma Pb}(-y)$$

$$\frac{d\sigma_{PbPb}^{0NXN}}{dy} = n_{0NXN}(\gamma, +y) \cdot \sigma_{\gamma Pb}(+y) + n_{0NXN}(\gamma, -y) \cdot \sigma_{\gamma Pb}(-y)$$

- Additional photon exchanges may lead to neutron emission

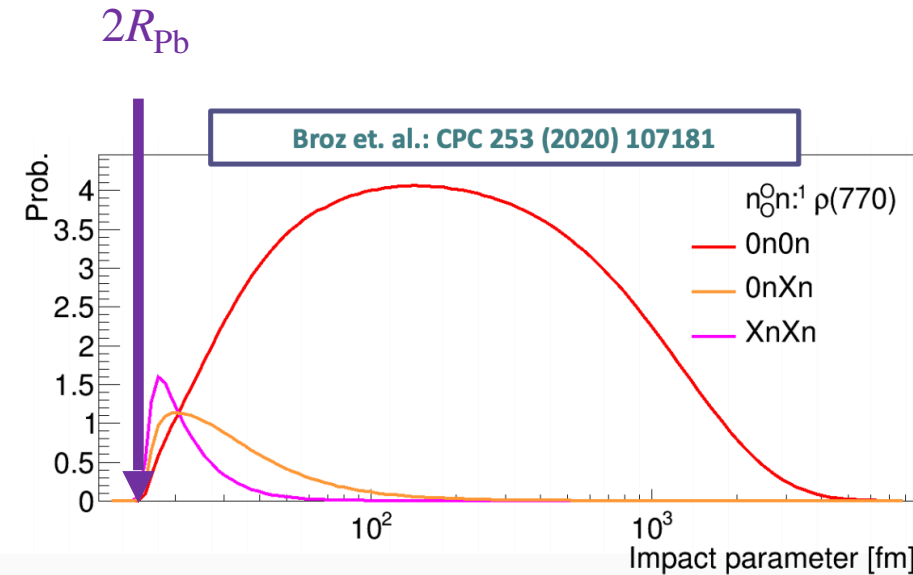
Guzey et al.,
Eur.Phys.J.C 74 (2014) 7, 2942

- Effectively leveraging on the impact parameter

Techniques for the photon direction ambiguity

Neutron emission:

- $x = \frac{M_{VM}}{\sqrt{s_{NN}}} \cdot e^{\pm y}$
- Ambiguity due to sign in the rapidity of the photon emitter $\rightarrow 10^{-2}, 10^{-5}$



- Using the neutron ZDCs on the A and C side to detect the neutrons!
- E.g. 0N0N: no neutrons on either ZDCs
- E.g. 0NXN: neutrons only on one side

$$\frac{d\sigma_{PbPb}^{0N0N}}{dy} = n_{0N0N}(\gamma, +y) \cdot \sigma_{\gamma Pb}(+y) + n_{0N0N}(\gamma, -y) \cdot \sigma_{\gamma Pb}(-y)$$

$$\frac{d\sigma_{PbPb}^{0NXN}}{dy} = n_{0NXN}(\gamma, +y) \cdot \sigma_{\gamma Pb}(+y) + n_{0NXN}(\gamma, -y) \cdot \sigma_{\gamma Pb}(-y)$$

- Additional photon exchanges may lead to neutron emission

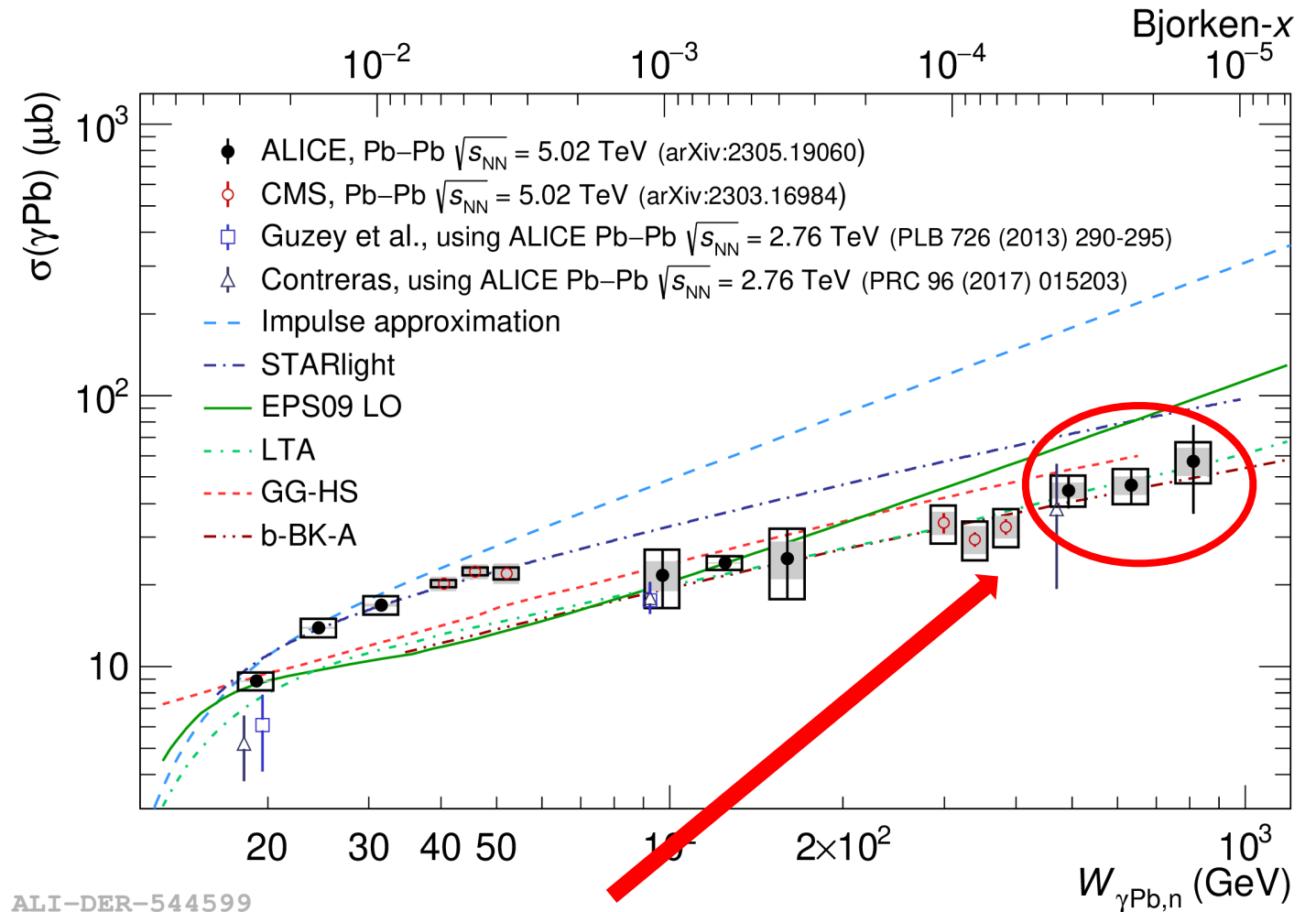
Guzey et al.,
Eur.Phys.J.C 74 (2014) 7, 2942

- Effectively leveraging on the impact parameter

Coherent J/ ψ with neutron emission

ALICE, JHEP 10 (2023) 119

- First measurement of the energy dependence of the photonuclear cross section down to Bjorken- $x \sim 10^{-5}$!
- At low- x data favours both saturation and shadowing models
- New Run 2 results probe unprecedented Bjorken- x region like no other LHC experiment!



Neutron emission extends the range in energy being explored by about 300 GeV!

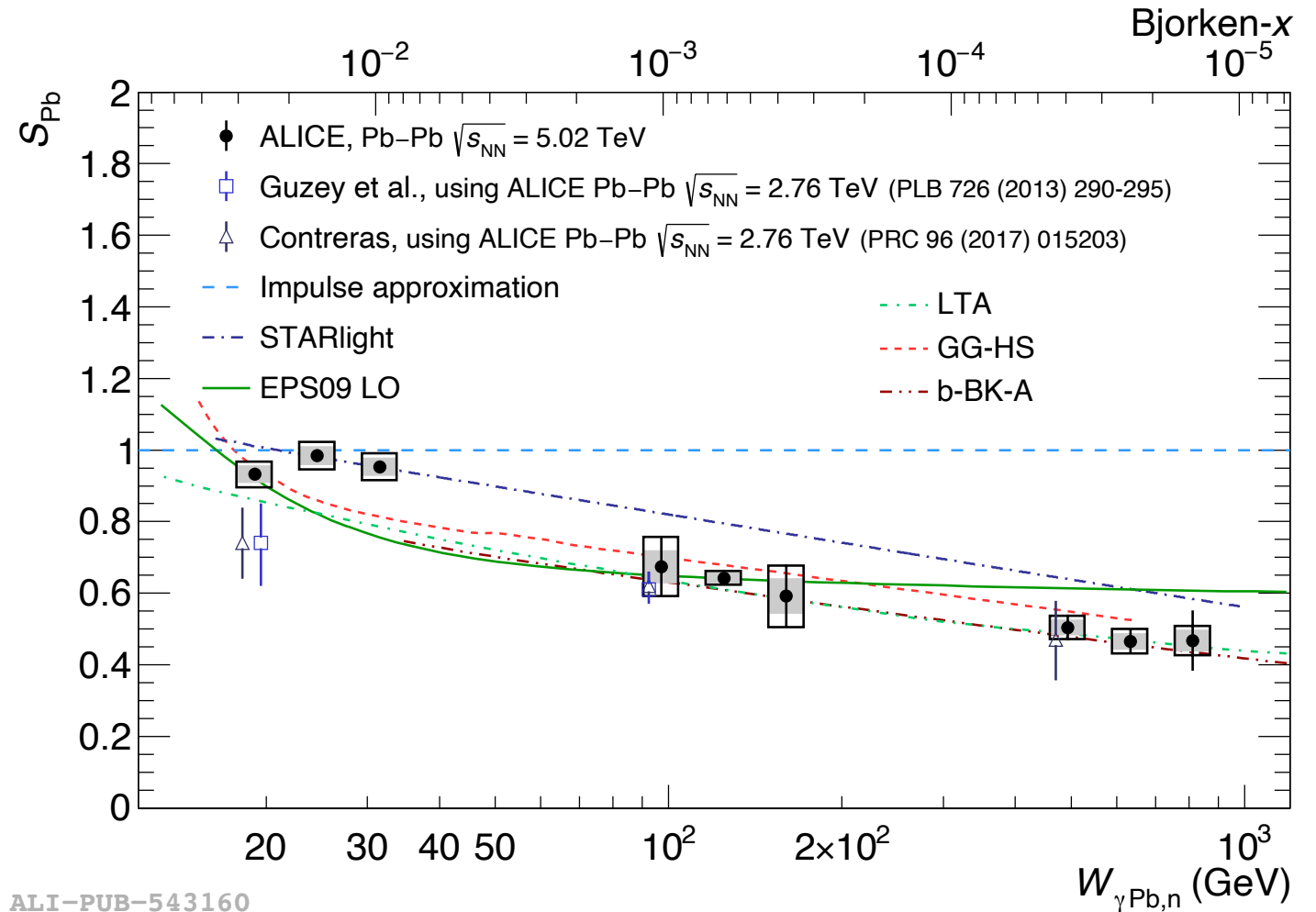
Coherent J/ψ with neutron emission

ALICE, JHEP 10 (2023) 119

- First measurement of the nuclear suppression factor at Bjorken- $x \sim 10^{-5}$!

$$S_{\text{Pb}}(y) = \sqrt{\frac{d\sigma}{dy}_{\text{data}} / \frac{d\sigma}{dy}_{\text{IA}}}$$

- At low- x data favours both saturation and shadowing models
- Additional theoretical uncertainty from impulse approximation \rightarrow dominates at low energies



ALI-PUB-543160

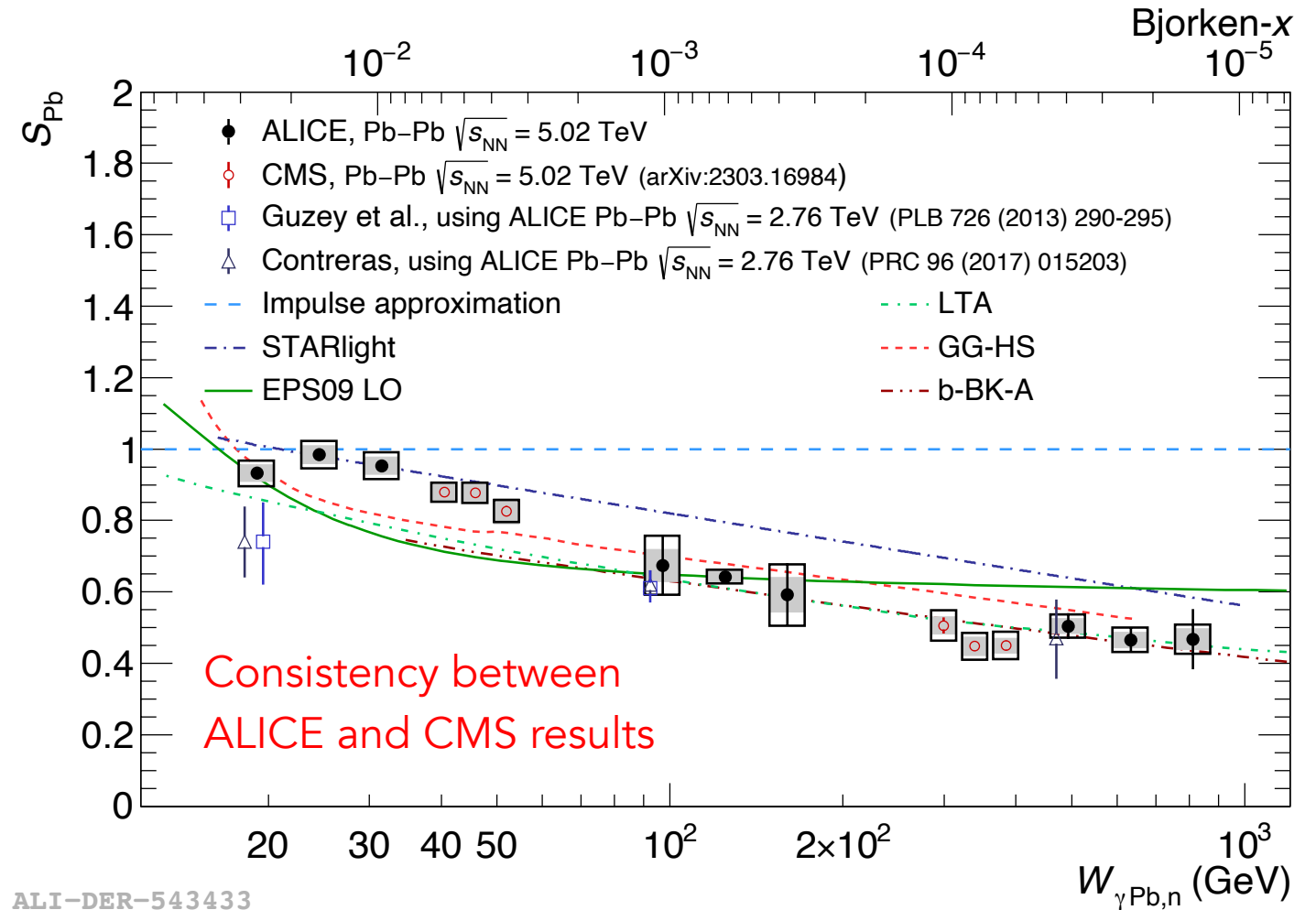
Coherent J/ψ with neutron emission

ALICE, JHEP 10 (2023) 119

- First measurement of the nuclear suppression factor at Bjorken- $x \sim 10^{-5}$!

$$S_{\text{Pb}}(y) = \sqrt{\frac{d\sigma}{dy}_{\text{data}} / \frac{d\sigma}{dy}_{\text{IA}}}$$

- At low- x data favours both saturation and shadowing models
- Additional theoretical uncertainty from impulse approximation \rightarrow dominates at low energies



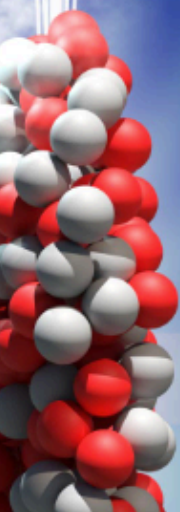
ALI-DER-543433

^{208}Pb

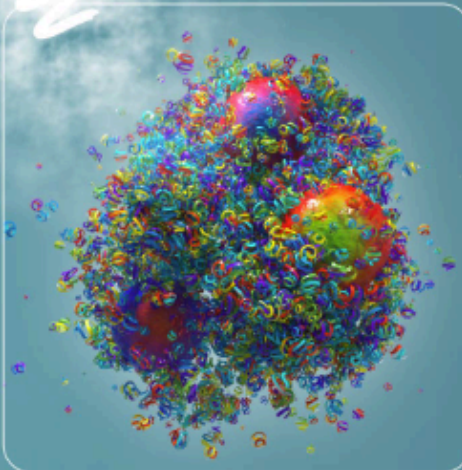
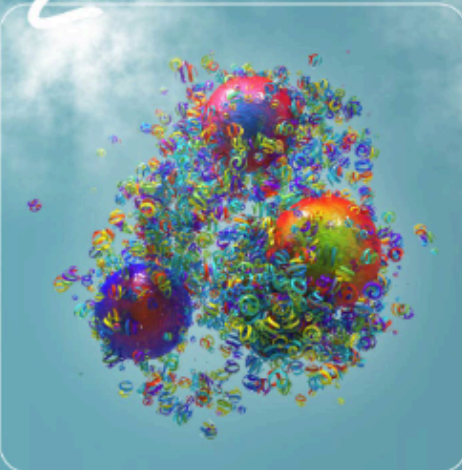
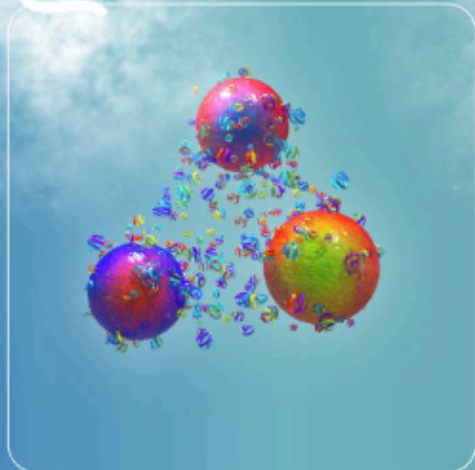


γ

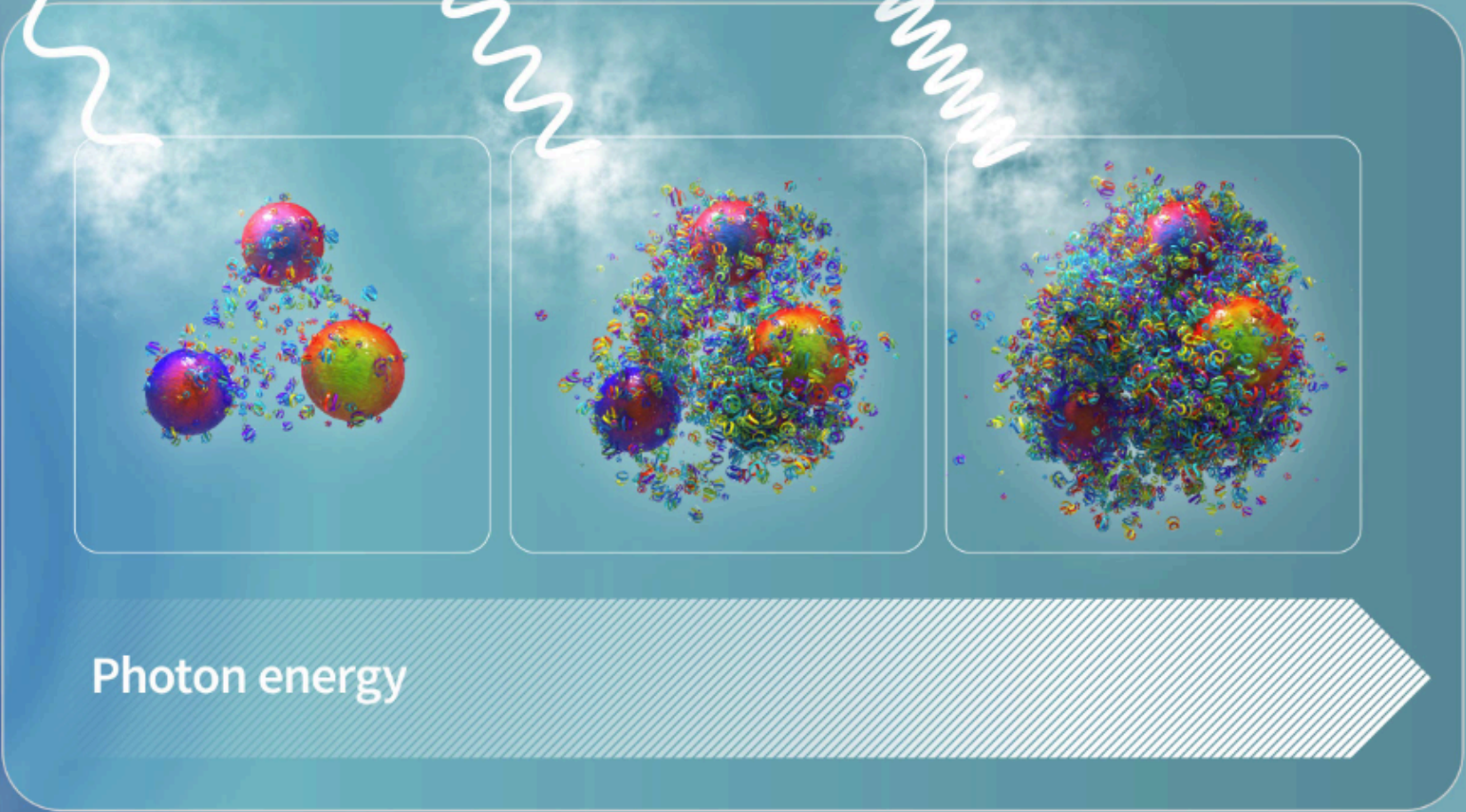
Vector meson



^{208}Pb

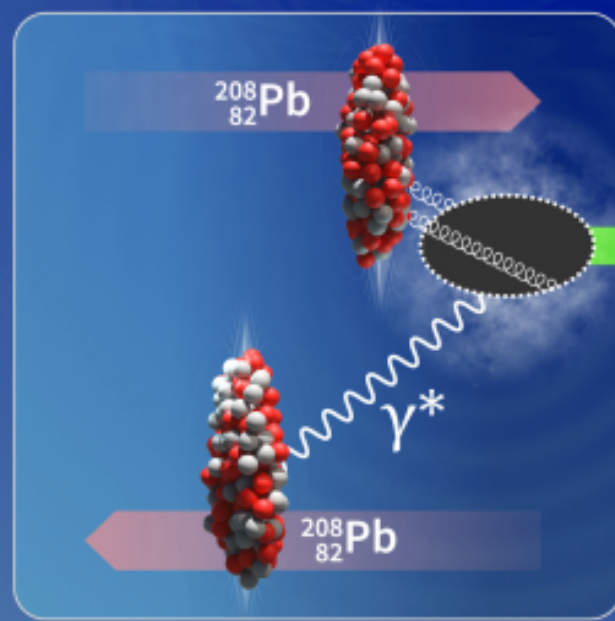
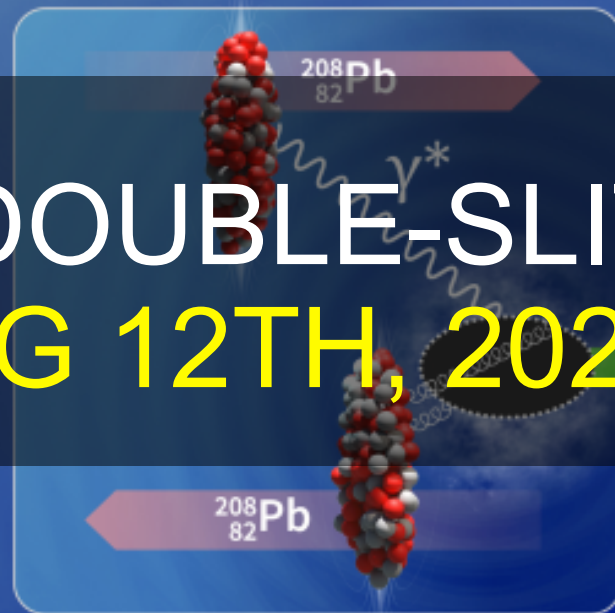
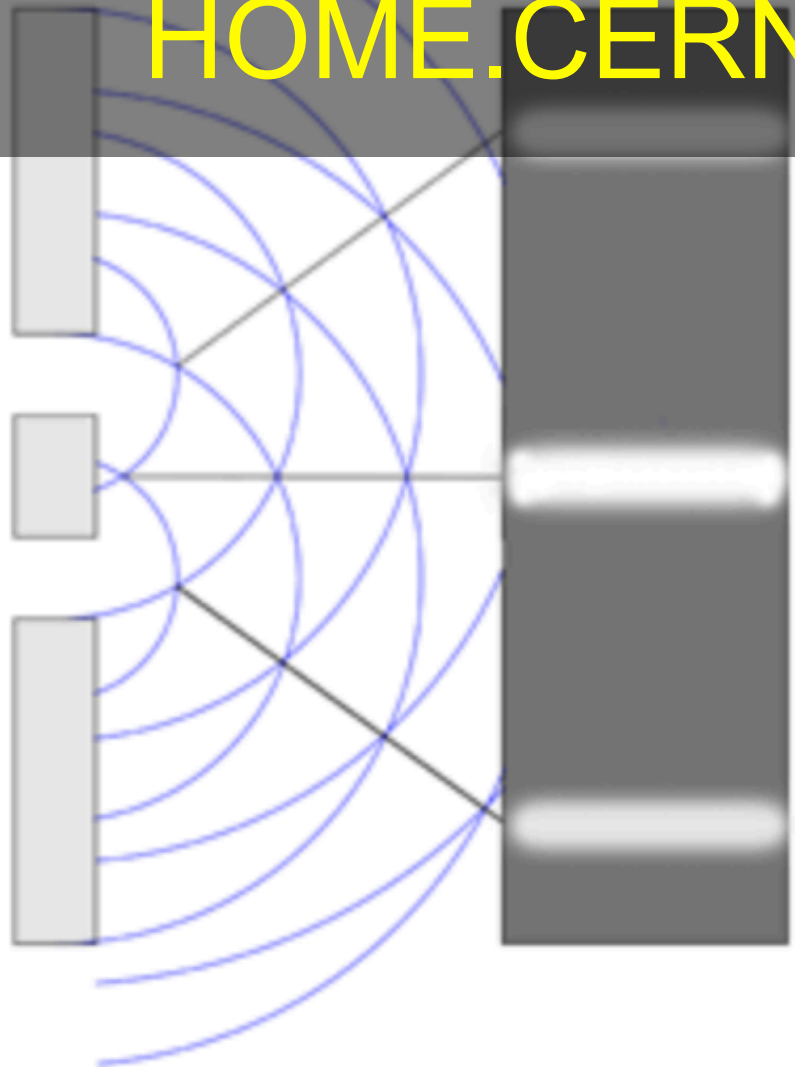


Photon energy

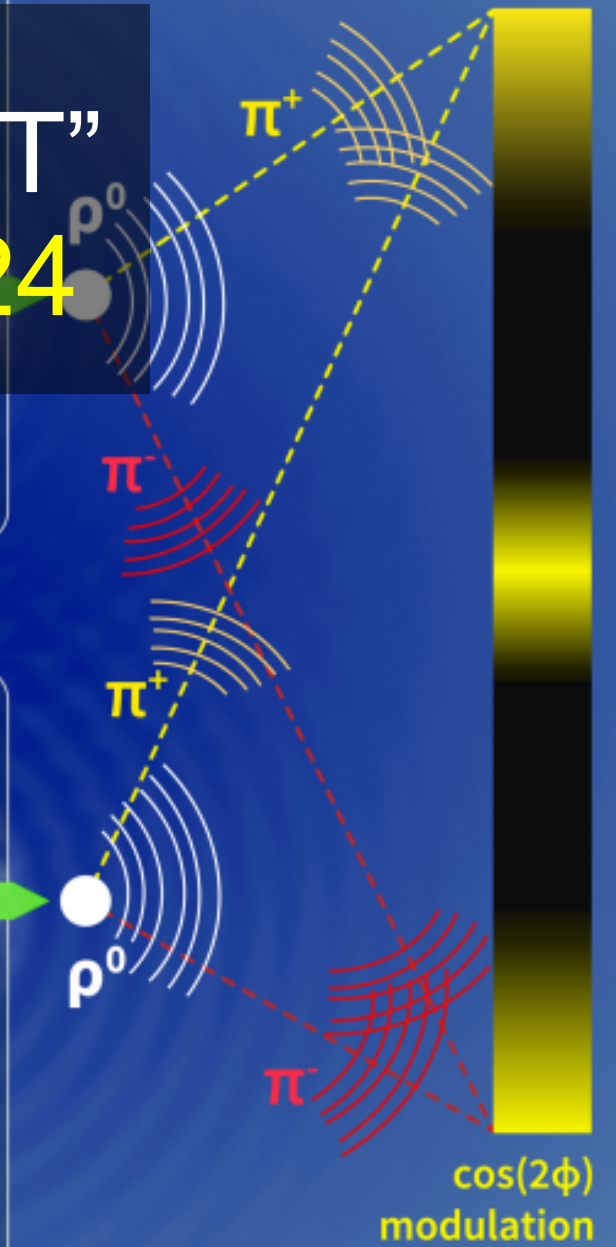


“ALICE DOES THE DOUBLE-SLIT”

HOME.CERN, AUG 12TH, 2024



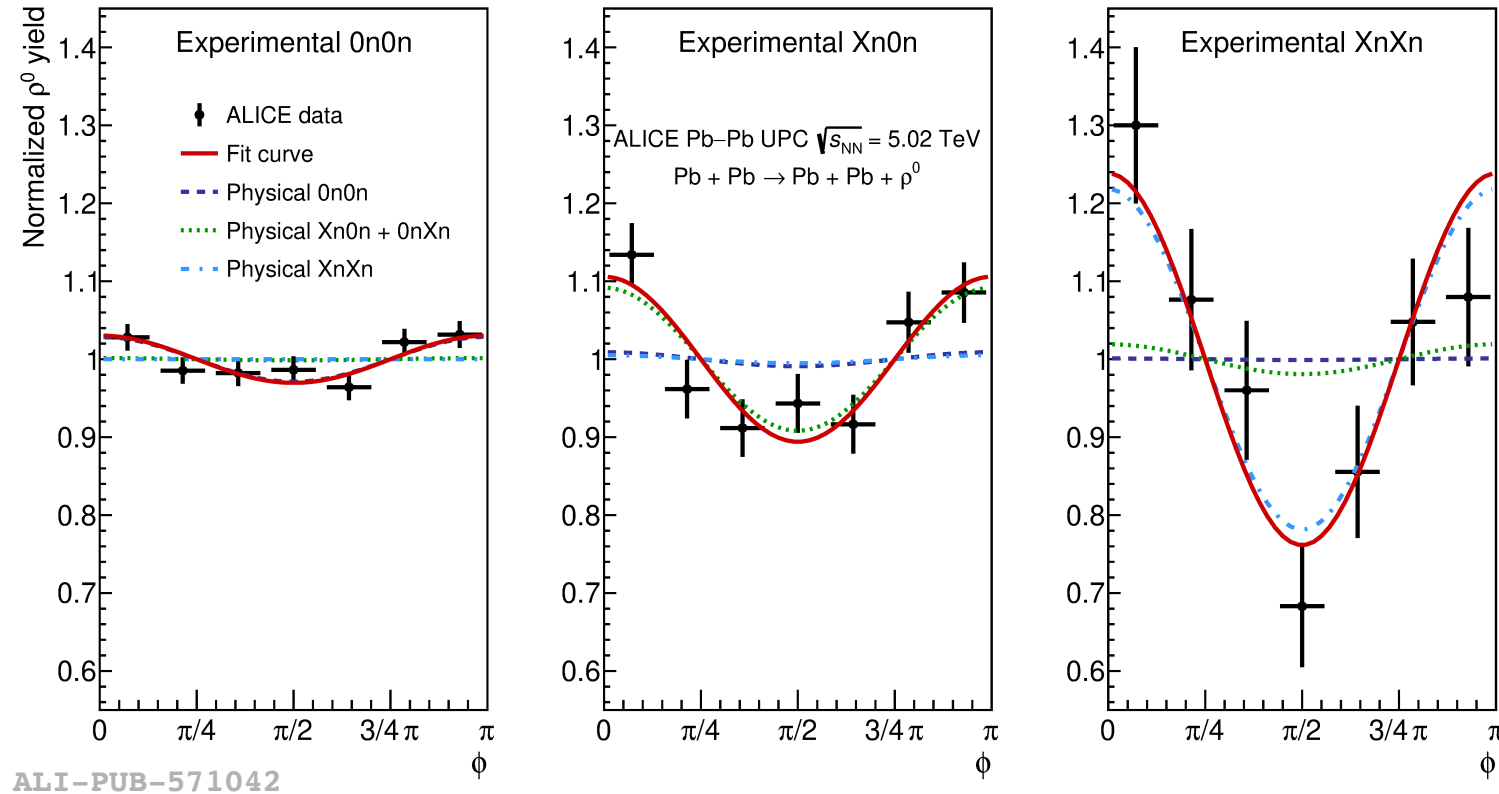
+



Coherent ρ^0 with neutron emission

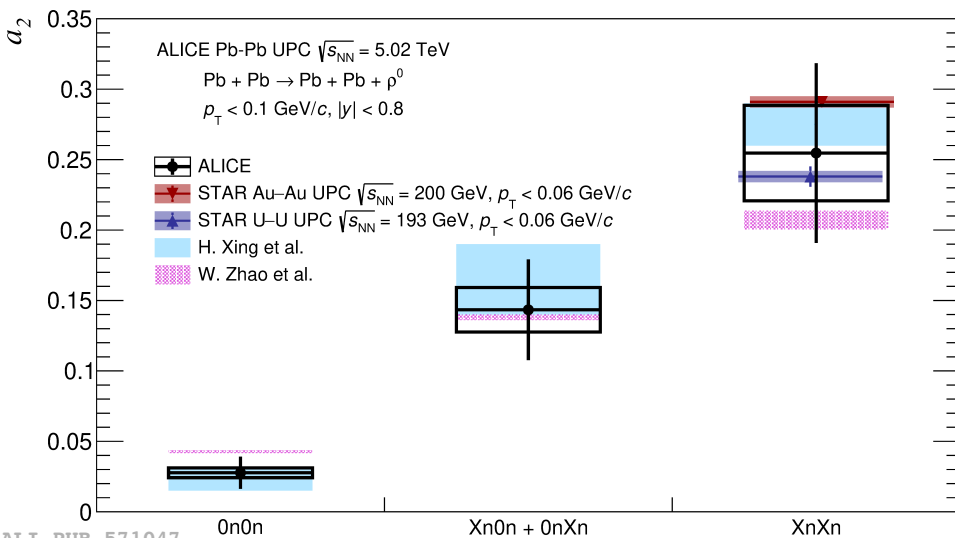
ALICE, arXiv:2405.14525 [nucl-ex], submitted to PLB

- Modulation increases as the impact parameter lowers
- ALICE results compatible with both theory and STAR results
- Modulation: linearly polarised photons + quantum interference at the fermi scale



<https://home.cern/news/news/physics/alice-does-double-slit>

Same technique: neutron emission classes \rightarrow impact parameter range



ALICE IN THE FUTURE UPGRADES IN RUN 3 AND 4



ALICE in Run 3 and 4

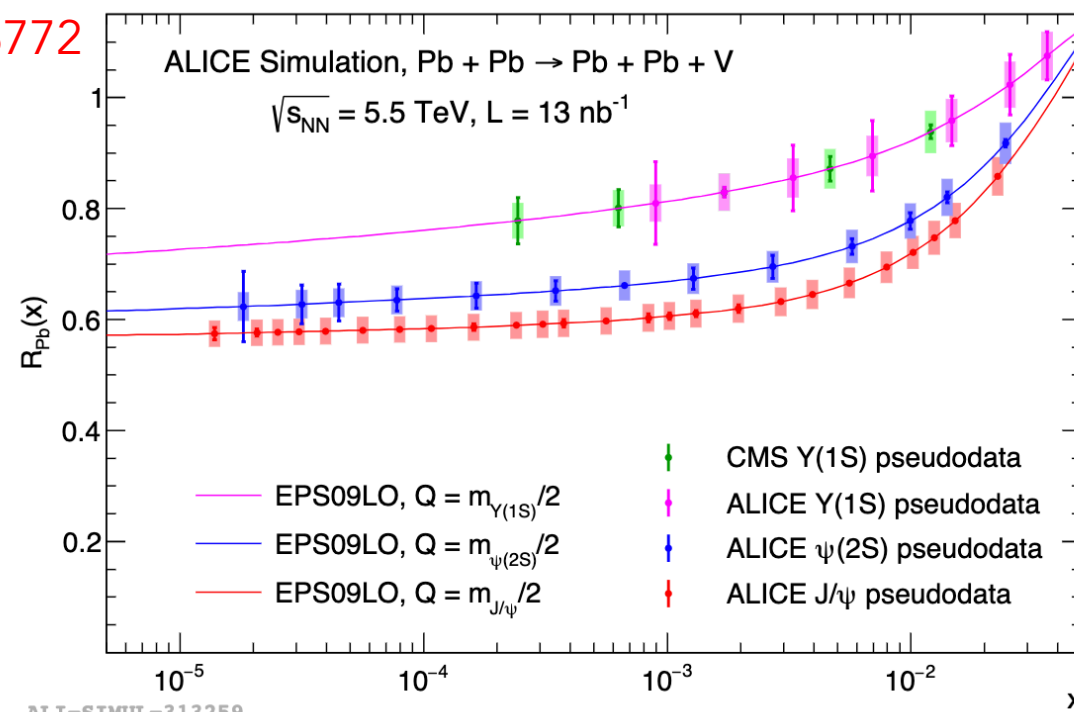
- Significant increase in integrated lumi from 1 nb^{-1} for Run 2 to 13 nb^{-1} for Run 3 and Run 4 together
- Great increase in statistics with continuous readout
- Uncertainties for nuclear suppression factor expected to be at the level of 4%
 - Nuclear shadowing studied as a function of x and Q^2
- New measurements e.g. bottomonium states
- MFT in Run 3, FoCal in Run 4!

PbPb			
Meson	σ	Central 1	Forward 1
		Total	Total l
$\rho \rightarrow \pi^+ \pi^-$	5.2b	5.5 B	4.9 B
$\rho' \rightarrow \pi^+ \pi^- \pi^+ \pi^-$	730 mb	210 M	190 M
$\phi \rightarrow K^+ K^-$	0.22b	82 M	15 M
$J/\psi \rightarrow \mu^+ \mu^-$	1.0 mb	1.1 M	600 K
$\psi(2S) \rightarrow \mu^+ \mu^-$	$30 \mu\text{b}$	35 K	19 K
$Y(1S) \rightarrow \mu^+ \mu^-$	$2.0 \mu\text{b}$	2.8 K	880

CERN Yellow Rep. Monogr. 7
(2019) 1159-1410, arXiv

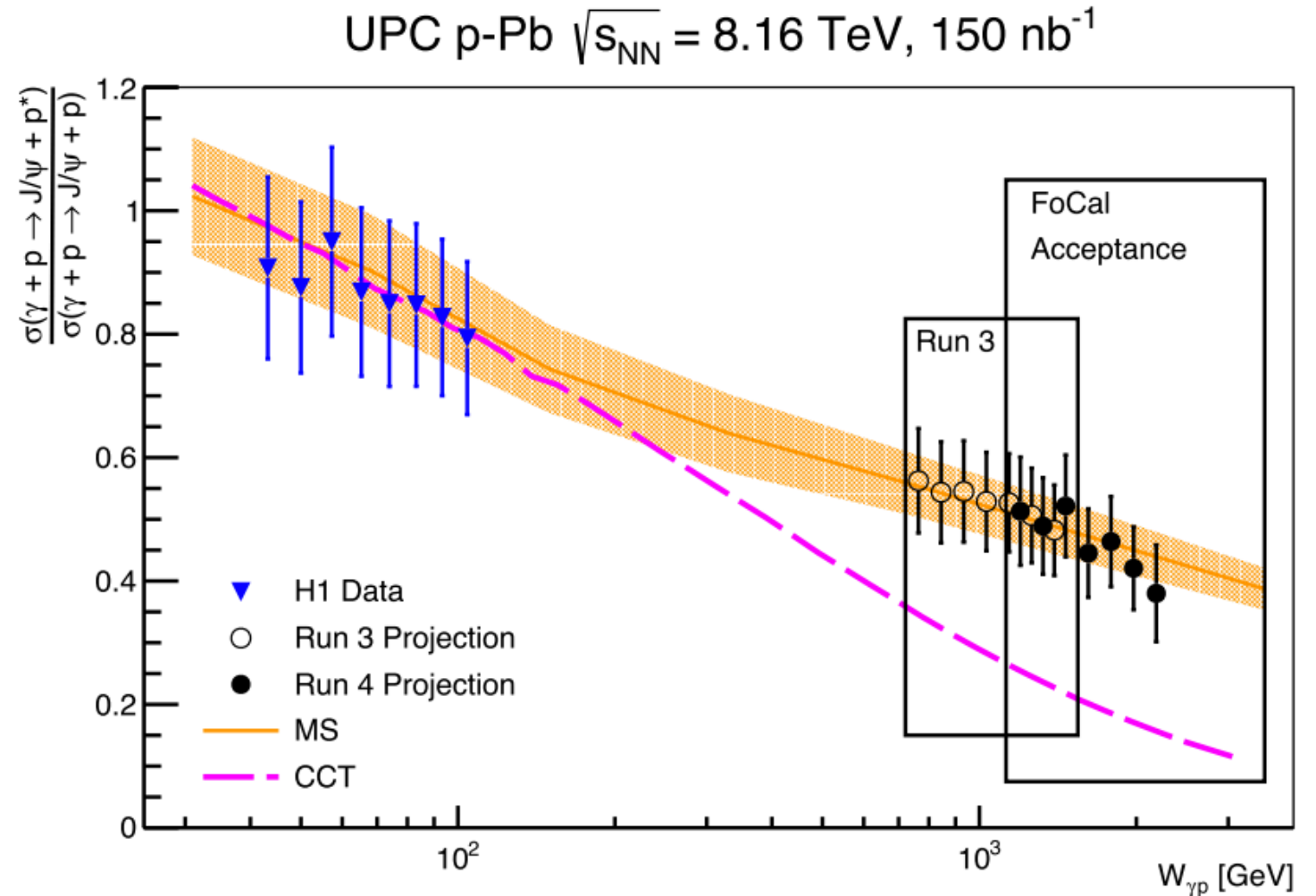
1812.06772

$|y| < 0.9$ $2.5 < |y| < 4$



Dissociative J/ψ in Run 3 and 4 (with FOCAL)

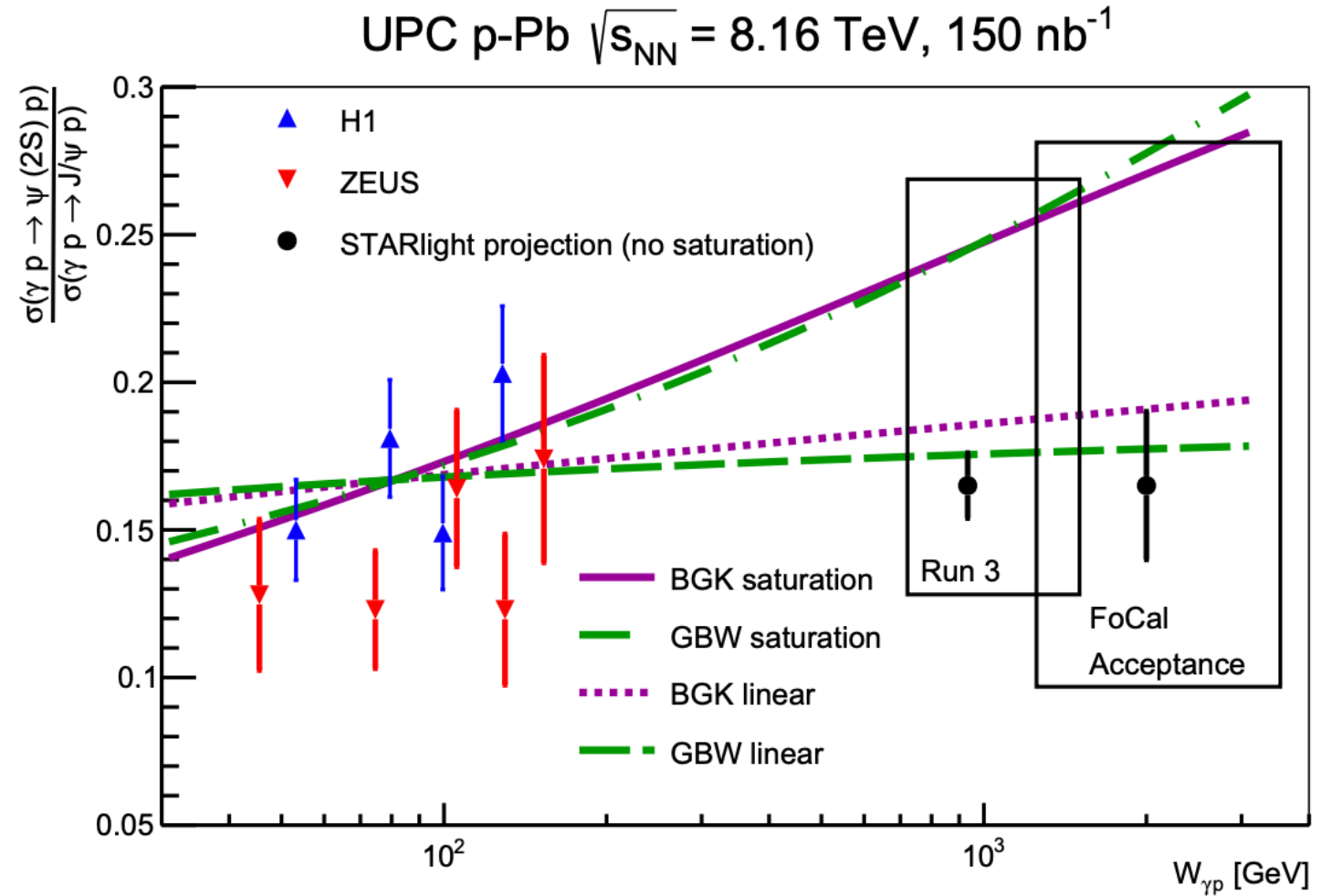
- Already in Run 3, but with FOCAL much easier to measure higher energies (using the channel $J/\psi \rightarrow ee$)
- CCT model features gluonic hotspots
- Significant reduction at higher energies would imply the onset of the saturation regime



A. Bylinkin, J. Nystrand, D. Tapia Takaki, 2023 *J. Phys. G: Nucl. Part. Phys.* **50** 055105

Exclusive J/ψ and ψ' in Run 3 and 4 (with FOCAL)

- The ratio is also a very sensitive observable
- Both Run 3 and 4 are needed to find the onset of the saturation regime



A. Bylinkin, J. Nystrand, D. Tapia Takaki, 2023 *J. Phys. G: Nucl. Part. Phys.* **50** 055105



Backup slides